(12) INTERNATIONAL APPLICATION PUBLISHED UNDER THE PATENT COOPERATION TREATY (PCT)

(19) World Intellectual Property Organization
International Bureau

(43) International Publication Date
06 April 2023 (06.04.2023)

WIPO | PCT

(10) International Publication Number
WO 2023/056261 A1

(51) International Patent Classification:
A61F 2/30 (2006.01) *A61B 5/055* (2006.01)
A61B 34/10 (2016.01) *A61B 34/30* (2016.01)
A61B 34/20 (2016.01) *G06N 20/00* (2019.01)
A61B 90/00 (2016.01) *G06T 1/00* (2006.01)
G06N 3/04 (2023.01)

(21) International Application Number:
PCT/US2022/077111

(22) International Filing Date:
27 September 2022 (27.09.2022)

(25) Filing Language: English

(26) Publication Language: English

(30) Priority Data:
63/250,906 30 September 2021 (30.09.2021) US

(71) Applicant: **MICROPORT ORTHOPEDICS HOLDINGS INC.** [US/US]; 5677 Airline Road, Arlington, TN 38002 (US).

(72) Inventors: **HARRIS, Brian, R.**; 5677 Airline Road, Arlington, TN 38002 (US). **BOWMAN, Fred, W.**; 5677 Airline Road, Arlington, TN 38002 (US).

(74) Agent: **HORNUNG, Robert, J.**; 5677 Airline Road, Arlington, TN 38002 (US).

(81) Designated States *(unless otherwise indicated, for every kind of national protection available)*: AE, AG, AL, AM, AO, AT, AU, AZ, BA, BB, BG, BH, BN, BR, BW, BY, BZ, CA, CH, CL, CN, CO, CR, CU, CV, CZ, DE, DJ, DK, DM, DO, DZ, EC, EE, EG, ES, FI, GB, GD, GE, GH, GM, GT, HN, HR, HU, ID, IL, IN, IQ, IR, IS, IT, JM, JO, JP, KE, KG, KH, KN, KP, KR, KW, KZ, LA, LC, LK, LR, LS, LU, LY, MA, MD, ME, MG, MK, MN, MW, MX, MY, MZ, NA, NG, NI, NO, NZ, OM, PA, PE, PG, PH, PL, PT, QA, RO,

WO 2023/056261 A1

(54) Title: SYSTEMS AND METHODS OF USING PHOTOGRAMMETRY FOR INTRAOPERATIVELY ALIGNING SURGICAL ELEMENTS

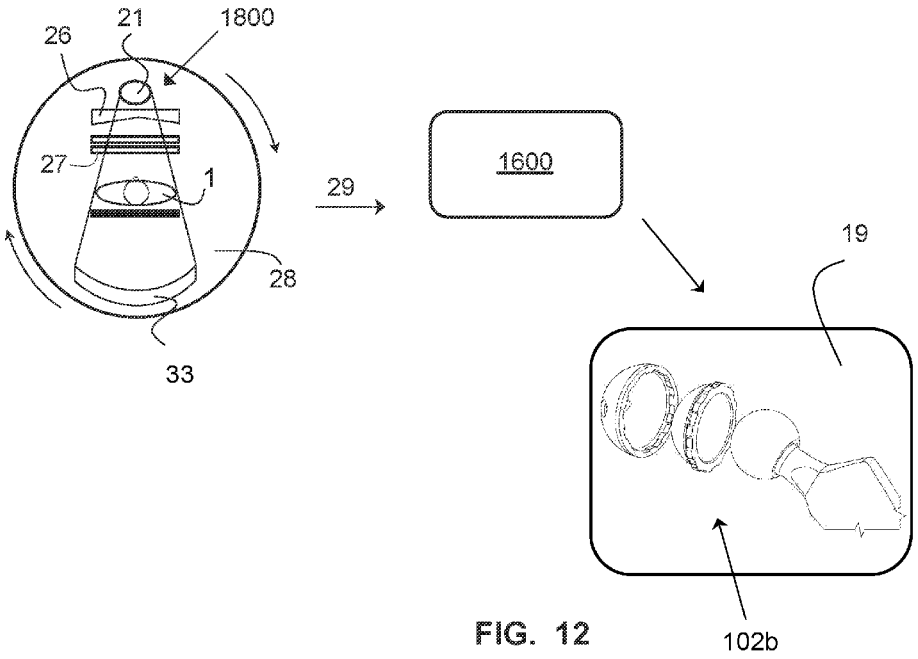

FIG. 12

(57) Abstract: Systems and methods for ascertaining a position of an orthopedic element in space comprising: capturing a first and second images of an orthopedic element in different reference frames using a radiographic imaging technique, detecting spatial data defining anatomical landmarks on or in the orthopedic element using a deep learning network, applying a mask to the orthopedic element defined by an anatomical landmark, projecting the spatial data from the first image and the second image to define volume data, applying the deep learning network to the volume data to generate a reconstructed three-dimensional model of the orthopedic element; and mapping the three-dimensional model of the orthopedic element to the spatial data to determine the position of the three-dimensional model of the orthopedic element in three-dimensional space.

[Continued on next page]

RS, RU, RW, SA, SC, SD, SE, SG, SK, SL, ST, SV, SY, TH, TJ, TM, TN, TR, TT, TZ, UA, UG, US, UZ, VC, VN, WS, ZA, ZM, ZW.

(84) **Designated States** *(unless otherwise indicated, for every kind of regional protection available)*: ARIPO (BW, GH, GM, KE, LR, LS, MW, MZ, NA, RW, SD, SL, ST, SZ, TZ, UG, ZM, ZW), Eurasian (AM, AZ, BY, KG, KZ, RU, TJ, TM), European (AL, AT, BE, BG, CH, CY, CZ, DE, DK, EE, ES, FI, FR, GB, GR, HR, HU, IE, IS, IT, LT, LU, LV, MC, MK, MT, NL, NO, PL, PT, RO, RS, SE, SI, SK, SM, TR), OAPI (BF, BJ, CF, CG, CI, CM, GA, GN, GQ, GW, KM, ML, MR, NE, SN, TD, TG).

Declarations under Rule 4.17:

— *as to the identity of the inventor (Rule 4.17(i))*
— *as to applicant's entitlement to apply for and be granted a patent (Rule 4.17(ii))*
— *as to the applicant's entitlement to claim the priority of the earlier application (Rule 4.17(iii))*

Published:

— *with international search report (Art. 21(3))*

SYSTEMS AND METHODS OF USING PHOTOGRAMMETRY FOR INTRAOPERATIVELY ALIGNING SURGICAL ELEMENTS

BACKGROUND OF THE INVENTION

1. Reference to Related Application

[0001] This application claims the benefit of priority to U.S. Provisional Application No. 63/250,906 filed on September 30, 2021. The disclosure of this related application is hereby incorporated into this disclosure in its entirety.

2. Technical Field

[0002] The present disclosure relates generally to the field of orthopedic joint replacement surgeries and more particularly to using photogrammetry and three-dimensional ("3D") reconstruction techniques to aid surgeons and technicians in planning and executing orthopedic surgeries.

3. Related Art

[0003] An objective of hip replacement surgeries is to restore the natural alignment and range of motion of the patient's pre-diseased hip. However, this objective can be difficult to achieve in practice, because hips comprise not only the articulating bones but also a variety of soft tissue, including cartilage, muscle, ligaments, and tendons. In all hip arthroplasties, and especially in minimally invasive hip arthroplasties , the presence of these soft tissues can severely limit the surgeon's visual field. This problem is even more pronounced in patients with a high body mass index.

[0004] In a hip arthroplasty, the pelvis itself is enclosed nearly entirely in soft tissue. In a minimally invasive procedure, the main incision eventually exposes the junction of the acetabulum and the proximal femoral head, but this main incision typically directs the surgeon's view across the margin (*i.e.,* perimeter) of the acetabulum. A portal incision extending through one or more quadriceps muscles of the operative leg may align with the concave face of the acetabulum, but the proximal end of the femur must be dislodged and rotated away from the acetabulum to expose this view.

[0005] To complicate matters further, the visual field of the operative area through a portal incision is generally much more limited than the visual field through the main incision. An endoscopic camera may be placed through the portal incision to capture an image of the concave acetabular surface, but the concave surface of the acetabulum lacks boney markers (*i.e.*, landmarks) that can be used to indicate the position of the acetabulum and pelvis reliably. Furthermore, any movement of the femur will likely translate to the pelvis through the connective soft tissue, thereby undermining the usefulness of any images captured by the endoscopic camera. Use of an endoscopic camera therefore would needlessly prolong the procedure and have very limited effectiveness in accurately reflecting the position of the acetabulum relative to the proximal femur.

[0006] Artificial hip implants typically comprise an acetabular shell, which the surgeon places into a reamed acetabulum of the hip. The acetabular shell may house a liner that functions essentially as a bearing with the generally spherically shaped head of the femoral component. The femoral component generally comprises a stem, a neck, and the head. When installed, the stem is inserted into a resected and reamed proximal end of the femur. The neck connects a proximal end of the stem to the head. The head in turn, is placed in the artificial acetabular cup, and commonly is disposed against the liner of the acetabular cup.

[0007] Because the surgeon's field of view of the surgical area is so often obstructed by soft tissue, surgeons have relied upon external indicia in the past to try to estimate the proper alignment of the acetabular cup in the acetabulum. US. Pat. Pub. No. 2013/0165941 to Murphy is one such example. Other providers offered positioning guides that comprised external horizonal and vertical positioning bars designed to resemble the axes of a Cartesian plane. To try to achieve an abduction angle of the acetabular cup of about 40 degrees ("°") to about 45°, the surgeon would position the placement guide roughly diagonally to the body longitudinal axis of the patient (*i.e.*, an imaginary center line of the body that extends from the patient's head to groin), such that a horizontal positioning bar would be disposed roughly parallel to the body longitudinal axis. To attempt to achieve an anteversion angle of about 10° to about 15°, the surgeon would lift the positioning device slightly along the vertical positioning bar relative to the body longitudinal axis.

[0008] These external indicia did not account for the patient's specific anatomy, nor did they account for movement of the pelvis relative to these indicia. For example, it is entirely possible that when a given patient is lying supine, the patient's left acetabulum may be positioned slightly lower than the patient's right acetabulum. Furthermore, many hip arthroplasty procedures require repositioning of the patient to make certain incisions or to access certain portions of the surgical area. As noted above, movement of the femur is likely to translate to the pelvis through the soft tissue. Given the need to reposition the patient multiple times throughout a standard hip

arthroplasty, it is unlikely that the pelvis will always be located within the suggested use parameters for existing acetabular cup positioning guides that rely upon external indicia.

[0009] Properly aligning, sizing, and installing the femoral component is even more difficult, given that allowing the surgeon to have a direct line of sight to the proximal femur requires dislocating (and therefore misaligning) the proximal femur from the acetabulum (or the acetabular cup as the case may be). As a result, many surgeons have relied upon sound and feel to approximate acceptable femoral stem placement. Both the femoral stem and the acetabular cup are impacted into their respective bones. A femoral stem that is too large could easily fracture the proximal femur. A femoral stem that is too small may subside into the intramedullary canal of the femur over time as the result of normal use. Subsidence can shorten the patient's gait and place undue pressure on the neck, head, and portions of the liner, thereby accelerating wear.

[0010] Additionally, even if the acetabular cup is placed in the reamed acetabulum at desirable angles of abduction and anteversion, and even if an adequately sized femoral stem is seated in the proximal femur, the position of the femoral component relative to the acetabular cup was previously not knowable using conventional technologies. Intraoperative fluoroscopy could be used to generate a two-dimensional ("2D") image of the femoral component relative to the acetabular component, but the fluoroscopic image lacked sufficient 3D information to ensure accurate alignment. For example, with classic fluoroscopy, the pelvic tilt was unknown. As such, the orientation of any boney landmarks on the pelvis was also unknown. Without being able to determine the orientation of the pelvis with precision, it was not possible to use fluoroscopy alone to accurately calculate the position of the natural pre-diseased joint line. Furthermore, prolonged use of fluoroscopy subjects the patient to excessive radiation.

[0011] Improper alignment of the femoral component's head relative to the acetabular cup could result in a shortening of the operative leg relative to the contralateral leg, dislocation of the head relative to the acetabular cup, and increased force loading on one part of the acetabular cup, liner, head, or neck (which thereby increases the rate of wear and reduced implant longevity). Any of these shortcomings can contribute to patient discomfort.

[0012] As a result, surgeons have had to remain content operating within a fairly large margin of error for acetabular cup placement. Despite the available tools and procedures, aligning a reconstructed hip in a typical hip arthroplasty is based on experience, educated guesses, and chance. This problem can be particularly pronounced in minimally invasive hip arthroplasties in part because the surgeon's field of view is so restricted.

SUMMARY OF THE INVENTION

[0013] Accordingly, there is a long felt but unresolved need to augment preoperative and intraoperative imaging technologies to accurately model the operative joint anatomy and artificial endoprosthetic implant when planning and executing hip arthroplasties.

[0014] The problems of limited surgeon visualization of the operative area in minimally invasive surgeries using currently available preoperative or intraoperative tools and techniques and the attendant problems of misalignment that such lack of visualization can cause can be mitigated by exemplary systems or methods for ascertaining a position of an orthopedic element in space comprising: using a deep learning network to identify and model an orthopedic element and a component of an endoprosthetic implant and to map the model of the orthopedic element and the model of the endoprosthetic implant to spatial data from an input of at least two separate two-dimensional ("2D") input images of a subject orthopedic element, wherein the first image of the at least two separate 2D input images is captured from a first transverse position, and wherein the second image of the at least two separate 2D input images is captured from a second transverse position offset from the first transverse position by an offset angle.

[0015] In exemplary embodiments, the input images can be radiographic images. Without being bound by theory, radiographs may be desirable because radiographs allow for in-vivo analysis that can account for external summation of passive soft tissue structures and dynamic forces occurring around the hip, including the effect of ligamentous restraints, load-bearing forces, and muscle activity.

[0016] Without being bound by theory, it is contemplated that by mapping the model of an orthopedic element and a model of a component of an endoprosthetic implant to spatial data, the position of the mapped and modeled orthopedic element can be calculated relative to the mapped and modeled implant component. If this system is applied to two or more orthopedic elements and two or more components of the endoprosthetic implant, the components of the endoprosthetic implants can be desirably implanted into their respective orthopedic elements at desirable positions and the respective endoprosthetic implant components can be desirably aligned relative to one another.

[0017] It is further contemplated that certain exemplary systems and methods described herein can be configured to accurately predict the desired size of an implant component relative to the adjacent orthopedic element.

[0018] It is still further contemplated that certain exemplary systems and methods described herein can be configured to accurately orient the placement of an endoprosthetic implant component relative to an orthopedic element in which the endoprosthetic implant component will be implanted.

BRIEF DESCRIPTION OF THE DRAWINGS

[0019] The foregoing will be apparent from the following more particular description of exemplary embodiments of the disclosure, as illustrated in the accompanying drawings. The drawings are not necessarily to scale, with emphasis instead being placed upon illustrating the disclosed embodiments.

[0020] **FIG. 1** is a simplified X-ray view of the front of a patient depicting an example endoprosthetic hip implant in the right hip and a natural left hip.

[0021] **FIG. 2** illustrates a surgeon's typical field of view in a minimally invasive hip arthroplasty.

[0022] **FIG. 3** is a perspective view of an example acetabular component disposed in a reamed acetabulum; **FIG. 3** depicts the principle of the abduction angle and the anteversion angle.

[0023] **FIG. 4** depicts a misaligned acetabular cup and a mis-sized femoral stem.

[0024] **FIG. 5** is a flow chart illustrating steps of an exemplary method.

[0025] **FIG. 6** is a flow chart illustrating steps of a further exemplary method.

[0026] **FIG. 7** is a schematic depiction of a system that uses a deep learning network to identify features (*e.g.*, anatomical landmarks) of a subject orthopedic element to generate a 3D model of the subject orthopedic element.

[0027] **FIG. 8** is a schematic depiction of a pinhole camera model used to convey how principles of epipolar geometry can be used to ascertain the position of a point in 3D space from two 2D images taken from different reference frames from calibrated image detectors.

[0028] **FIG. 9A** is an image of the subject orthopedic elements taken from the anterior-posterior ("A-P") position that shows an exemplary calibration jig.

[0029] **FIG. 9B** is an image of the subject orthopedic elements of **FIG. 9A** taken at about 45° clockwise from reference frame of **FIG. 9A** with the calibration jig.

[0030] **FIG. 9C** is an image of the subject orthopedic elements of **FIG. 9A** taken at about 45° counterclockwise from reference frame of **FIG. 9A** with the calibration jig.

[0031] **FIG. 10** is a schematic representation depicting how a convolutional neural network ("CNN") type deep learning network can be used to identify features (*e.g.*, anatomical landmarks), including the surface of a subject orthopedic element.

[0032] **FIG. 11** is an exploded view of a modeled endoprosthetic implant.

[0033] **FIG. 12** is a schematic representation of an exemplary system.

[0034] **FIG. 13** is a schematic representation of a system configured to generate a model of an orthopedic element and to align components of endoprosthetic implant components using two

or more tissue penetrating, flattened, input images taken of the same subject orthopedic element from calibrated detectors at an offset angle.

DETAILED DESCRIPTION OF THE PREFERRED EMBODIMENTS

[0035] The following detailed description of the preferred embodiments is presented only for illustrative and descriptive purposes and is not intended to be exhaustive or to limit the scope and spirit of the invention. The embodiments were selected and described to best explain the principles of the invention and its practical application. One of ordinary skill in the art will recognize that many variations can be made to the invention disclosed in this specification without departing from the scope and spirit of the invention.

[0036] Similar reference characters indicate corresponding parts throughout the several views unless otherwise stated. Although the drawings represent embodiments of various features and components according to the present disclosure, the drawings are not necessarily to scale and certain features may be exaggerated to better illustrate embodiments of the present disclosure, and such exemplifications are not to be construed as limiting the scope of the present disclosure.

[0037] Except as otherwise expressly stated herein, the following rules of interpretation apply to this specification: (a) all words used herein shall be construed to be of such gender or number (singular or plural) as such circumstances require; (b) the singular terms “a,” “an,” and “the,” as used in the specification and the appended claims include plural references unless the context clearly dictates otherwise; (c) the antecedent term “about” applied to a recited range or value denotes an approximation with the deviation in the range or values known or expected in the art from the measurements; (d) the words, “herein,” “hereby,” “hereto,” “hereinbefore,” and “hereinafter,” and words of similar import, refer to this specification in its entirety and not to any particular paragraph, claim, or other subdivision, unless otherwise specified; (e) descriptive headings are for convenience only and shall not control or affect the meaning of construction of part of the specification; and (f) “or” and “any” are not exclusive and “include” and “including” are not limiting. Further, the terms, “comprising,” “having,” “including,” and “containing” are to be construed as open-ended terms (*i.e.*, meaning “including but not limited to”).

[0038] References in the specification to “one embodiment,” “an embodiment,” “an exemplary embodiment,” *etc.*, indicate that the embodiment described may include a particular feature, structure, or characteristic, but every embodiment may not necessarily include the particular feature, structure, or characteristic. Moreover, such phrases are not necessarily referring to the same embodiment. Further, when a particular feature, structure, or characteristic is described in connection with an embodiment, it is submitted that it is within the knowledge of one skilled in

the art to affect such feature, structure, or characteristic in connection with other embodiments, whether explicitly described.

[0039] To the extent necessary to provide descriptive support, the subject matter and/or text of the appended claims are incorporated herein by reference in their entirety.

[0040] Recitation of ranges of values herein are merely intended to serve as a shorthand method of referring individually to each separate value falling within the range of any sub-ranges there between, unless otherwise clearly indicated herein. Each separate value within a recited range is incorporated into the specification or claims as if each separate value were individually recited herein. Where a specific range of values is provided, it is understood that each intervening value, to the tenth or less of the unit of the lower limit between the upper and lower limit of that range and any other stated or intervening value in that stated range of sub range thereof, is included herein unless the context clearly dictates otherwise. All subranges are also included. The upper and lower limits of these smaller ranges are also included therein, subject to any specifically and expressly excluded limit in the stated range.

[0041] It should be noted that some of the terms used herein are relative terms. For example, the terms, "upper" and, "lower" are relative to each other in location, *i.e.,* an upper component is located at a higher elevation than a lower component in each orientation, but these terms can change if the orientation is flipped

[0042] The terms, "horizontal" and "vertical" are used to indicate direction relative to an absolute reference, *i.e.,* ground level. However, these terms should not be construed to require structure to be absolutely parallel or absolutely perpendicular to each other. For example, a first vertical structure and a second vertical structure are not necessarily parallel to each other. The terms, "top" and "bottom" or "base" are used to refer to locations or surfaces where the top is always higher than the bottom or base relative to an absolute reference, *i.e.,* the surface of the Earth. The terms, "upwards" and "downwards" are also relative to an absolute reference; an upwards flow is always against the gravity of the Earth.

[0043] Orthopedic procedures frequently involve operating on a patient's joint. It will be understood that a joint typically comprises a multitude of orthopedic elements. It will further be appreciated that the exemplary methods and systems described herein can be applied to a variety of orthopedic elements. The examples described with reference to **FIGS. 1 – 4**, **9A – 9C**, and **11** relate to a hip joint for illustration purposes. It will be appreciated that the "orthopedic element" **100** referenced throughout this disclosure is not limited to the anatomy of a hip joint, but can include any skeletal structure or associated soft tissue, such as tendons, ligaments, cartilage, and muscle. A non-limiting list of example of skeletal orthopedic elements **100** includes any partial or complete

bone from a body, including but not limited to a femur, tibia, pelvis, vertebra, humerus, ulna, radius, scapula, skull, fibula, clavicle, mandible, rib, carpal, metacarpal, tarsal, metatarsal, phalange, or any associated tendon, ligament, skin, cartilage, or muscle. It will be appreciated that an example operative area **170** can comprise several subject orthopedic elements **100**. Likewise, it will be appreciated that an operative area **170** is not limited to the hip operative area that is used as the primary example herein, but rather can return to any area of a body that is the target of a surgical operation. This may include by non-limiting example, the knee, ankle, spine, shoulder, wrist, hand, foot, mandible, skull, rib, and phalanges.

[0044] **FIG. 1** is a simplified representation of an X-ray image of the front of an example patient's pelvis **110**. Both patient's right hip joint **101a** and left hip joint **101b** are shown. Both example hip joints **101a**, **101b** comprise a number of orthopedic elements **100**, including a femur **105**, an acetabulum (see **108** and **111**) of the pelvis **110**, and connective tissues. The depicted right hip joint **101a** (*i.e.*, the hip joint on the patient's right side, which is depicted on the left side of the page) shows an example endoprosthetic hip implant **102** that has been surgically installed into the patient. The depicted left hip joint **101b** shows an example natural hip joint for comparison.

[0045] Referring to the depicted right hip joint **101a**, the example endoprosthetic hip implant **102** generally comprises an acetabular component **103** and a femoral component **104**. It will be appreciated that endoprosthetic implants in general can comprise multiple components (*e.g.*, an acetabular component **103** and a femoral component **104**); these components in turn may be comprised of multiple subcomponents. In the depicted example, the acetabular component **103** typically comprises a generally hemispherical acetabular shell **106** and an inner liner **107**. The acetabular shell **106** is typically made from cobalt chrome, titanium, or other biocompatible metal. The inner liner **107** is typically made from a ceramic, metal, polymer, or other biocompatible material having a low coefficient of friction and a low wear rate.

[0046] To prepare the native acetabulum (see **108**) for the installation of the acetabular shell **106**, the surgeon first uses a hemispherical reamer to create a generally concave surface in the patient's native acetabulum **108** to define a "reamed acetabulum" **111**. The reamed acetabulum **111** is generally complementary to the convex outer surface **109** of the acetabular shell **106**. The outer surface **109** of the acetabular shell **106** is usually roughened to facilitate engagement to the reamed acetabulum **111**. The roughened surface is also thought to promote osteogenesis into the spaces of the roughened surface, thereby increasing the strength of the bond over time.

[0047] The inner liner **107** typically sits adjacent to an inner concave surface **112** of the acetabular shell **106**, when the inner liner **107** is in its assembled and installed configuration. The inner liner **107** generally functions as a bearing against which the femoral head **113** of the femoral component **104** articulates once installed.

[0048] The femoral component **104** typically comprises the femoral stem **115** having a distal stem end **115a** that is distally disposed from a proximal stem end **115b**, a neck **116** having a distal neck end **116a** engaging the proximal stem end **115b**. The neck **116** extends to a head end **116b**. A generally spherically shaped artificial femoral head **113** is disposed at the head end **116b** of the neck **116** in an assembled configuration. In certain exemplary embodiments, the neck **116** can be selectively detachable from the proximal stem end **115b**. Such selectively detachable necks **116** can be known as "modular necks."

[0049] It will be appreciated that the acetabular component **103** and the femoral component **104**, and the subcomponents that comprise the acetabular component **103** or the femoral component **104** (*e.g.*, the acetabular shell **106**, inner liner **107**, any fixation fasteners, the femoral stem **115**, artificial femoral head **113**, *etc.*) are typically provided in one or more surgical kits in an uninstalled and unassembled configuration. In an uninstalled and unassembled configuration, a component or subcomponent does not physically engage another component or subcomponent. Stated another way force is not directly transferred from one component or subcomponent to another component or subcomponent in an uninstalled and unassembled configuration. In as assembled configuration, the components or subcomponents physically contact one another and force can be transferred through two or more proximally disposed components or subcomponents. In an assembled and installed configuration, the components or subcomponents are in the assembled configuration and are also surgically implanted into the patient.

[0050] For comparison, the depicted left hip joint **101b** shows the natural femoral head **126** at the proximal end of the femur **105**. The natural femoral head **126** is disposed within the natural acetabulum **108** of the pelvis **110**. Articular cartilage **123** coats the articular surface of both the healthy femoral head **126** and the healthy acetabulum **108**.

[0051] There are many surgical approaches to a typical hip arthroplasty, but most minimally invasive procedures begin with the surgeon making a six to eight centimeters ("cm") incision in the operative leg that is radially proximate to the hip joint capsule. Various muscles and tendons are then retracted with surgical instruments to eventually expose the joint capsule. The capsule is then pierced, and the surgeon dislocates the natural femoral head **126** from the natural acetabulum **108**.

[0052] Femoral preparation involves resecting and removing the natural femoral head **126** from the femur **105**. After the natural femoral head **126** is removed, the surgeon may then drill a canal into the intramedullary space of newly exposed proximal end **105b** of the femur **105**. The surgeon may then use a femoral broach to expand the space in the intramedullary canal needed to accommodate the femoral stem **115**. Trial stems may be used to test the sizing and positioning of

the femoral component **104**. Trial components generally have the same dimensions as the actual implant components, but the trial components are designed to be installed and removed more easily.

[0053] Acetabular preparation involves reaming the natural acetabulum **108** to define a reamed acetabulum **111**. The goal is to create a generally uniform hemispherical space that is complementary to the generally hemispherical outer surface **109** of the acetabular shell **106**. Trial acetabular components can be used to try to test the alignment of the acetabular component **103** relative to the femoral component **104**, but visibility is limited and the nature of the procedure typically does not permit exhaustive testing of the alignment. Furthermore, because visibility is limited, there is a chance that the actual implant components **103**, **104** will not be oriented in exactly the same way as the trial components.

[0054] It will be appreciated that there are a variety of surgical approaches for a typical total hip arthroplasty (*e.g.*, some surgeons choose to approach the hip posteriorly, while other choose to approach the hip joint laterally or anteriorly). **FIG. 2** illustrates and exemplifies a surgeon's typical field of view of a typical hip arthroplasty operative area **170** through the main incision. Several retractors **14**, **16** (which can include a Hohmann retractor or a Cobb elevator in some procedures) are used to retract the fascia **11** that is disposed between the area of the initial incision and the hip joint capsule. An electrocautery instrument **40** can be used to resect and cauterize tissue and to prevent excessive bleeding. The natural femoral head **126** is also shown for reference.

[0055] **FIG. 2** illustrates how the six to eight cm main incision of the operative area **170**, the location of the hip joint (see **101a**, **101b**) relative to the point of incision, and the presence of typical surgical instrumentation (*e.g.*, retractors **14**, **16**, mallets, broaches, reamers, pins, implant components, *etc.*) can significantly interfere with the surgeon's already limited field of view. This problem, which can be exacerbated by trying to align the acetabular component **103** and the femoral component **104** of the endoprosthetic hip implant **102** relative to external indicia that are divorced from the orientation of the target's implantation anatomy (*e.g.*, the reamed acetabulum **111** or the resected proximal femur **105** in this hip example), can lead to inaccurate alignment of the implant components **103**, **104** relative to the bones into which they are implanted, and relative to each other. This in turn can contribute to the risk of implant dislocation, non-optimal force distribution, faster wear, failure of the implant, altered gait, general patient discomfort, and the need for further revision surgeries which suffer from the same limitations.

[0056] **FIG. 3** is a perspective view of an example acetabular component **103** disposed in a reamed acetabulum **111**. Although the abduction angle **α** and the anteversion angle **υ** are depicted with reference to the acetabular component **103**, it will be appreciated that the femoral component **104** is also disposed at an abduction angle **α** and an anteversion angle **υ** in the proximal

femur **105**. The abduction angle **α** and an anteversion angle **υ** of a component of an endoprosthetic implant (*e.g.*, the acetabular component **103** and the femoral component **104**) relative to the orthopedic element (*e.g.*, the pelvis **110** and **105** proximal femur respectively) into which the component of the endoprosthetic implant is implanted can be calculated and determined by those having ordinary skill in the art.

[0057] It will be appreciated that a "component of an endoprosthetic implant" can vary based upon the type of endoprosthetic implant and the type of operative area **170**. For example, when the operative area **170** is a hip, a "component of an endoprosthetic implant" can be selected from a group comprising an acetabular component **103**, a femoral component **104**, a trial construct, instrumentation used in or to facilitate the installation of the endoprosthetic implant or trial implants in the patient in the installed position, or combinations thereof. In embodiments where the operative area **170** is a knee, a "component of an endoprosthetic implant" can be a femoral component of an endoprosthetic knee implant, a tibial component of an endoprosthetic knee implant, a trial construct, instrumentation used in or to facilitate the installation of the endoprosthetic implant or trial implants in the patient in the installed position, or combinations thereof.

[0058] To illustrate the principle of the abduction angle **α** of the acetabular component **103** relative to the pelvis **110** more clearly, the soft tissue has been omitted in **FIG. 3**. The abduction angle **α** can be measured by several ways known by those having ordinary skill in the art. One such way of visualizing the abduction angle **α** of the acetabular component **103** is by drawing a diameter line **D** extending through the diameter of the rim of the acetabular shell **106** on a coronal plane **CP** relative to a generally horizontal medial-lateral reference line **R** that is co-planar with the coronal plane **CP** of the diameter line **D**. In **FIG. 3**, the reference line **R** is shown connecting the distalmost portions of the right and left ischia **117a**, **117b**; however, it will be appreciated that other reference markers may be used provided that the reference line **R** extends horizontally, medial-laterally, and co-planarly coronally with the diameter line **D**.

[0059] A shell plane **SP** is also shown extending coplanar through the rim **2** of the acetabular shell **106**. Aligning the acetabular shell **106** in three dimensional space can be thought to involve the selection of the proper compound angle, the compound angle comprising the abduction angle **α** and the anteversion angle **υ**. The shell plane **SP** is shown to depict the concept of acetabular shell alignment in three dimensions more clearly. It will be appreciated that the diameter line **D**, coronal plane **CP**, shell plane **SP**, and the medial-lateral reference line **R** are geometric reference elements that are depicted to illustrate the concept of the abduction angle **α** and acetabular alignment generally. These geometric reference elements need not be visible in practice.

[0060] Many acetabular shells **106** are designed to be installed in the reamed acetabulum **111** at an abduction angle **α** of about 30° to about 50°. However, this wide margin underscores the

difficulty in properly aligning an acetabular shell **106** in the reamed acetabulum **111** using conventional methods. Furthermore, the general guidance of having an abduction angle **α** of about 30° to about 50° does not account for variability in particular patients.

[0061] **FIG. 3** also illustrates the concept of the anteversion angle **υ**. The anteversion angle **υ** can be calculated by several ways known to those having ordinary skill in the art. One such way to visualize the anteversion angle **υ** of the acetabular shell **106** is to imagine the anteversion angle **υ** as the rotation of the acetabular shell **106** around the center diameter line **D** used in the abduction angle **α** visualization. A typical acetabular shell **106** may have an anteversion angle **υ** in a range of about 10° to about 30°, or about 10° to about 20°, or about 15° to about 25°. It will be appreciated that in practice, the alignment of the acetabular shell **106** within the reamed acetabulum **111** is a compound angle comprising both the abduction angle **α** and the anteversion angle **υ**. Likewise, the alignment of the femoral stem **115** within the intramedullary bore **119** is a compound angle comprising both the abduction angle **α** and the anteversion angle **υ**.

[0062] The anteversion angle **υ** of the femoral stem **115** typically has the same range of values of the anteversion angle **υ** of the acetabular shell **106** (*i.e.*, a range of about 10° to about 30°, or about 10° to about 20°, or about 15° to about 25°) because having a femoral stem **115** that aligns with an acetabular shell **106** along a common angle of anteversion (or anteversion plane) is one of the alignment parameters of a properly aligned endoprosthetic hip implant **102**. Placing the femoral stem **115** in the intramedullary canal of the proximal femur **105** such that the longitudinal axis of the femoral stem is co-linear with the anatomical axis of the femur **105** into which the femoral stem **115** is placed is another alignment parameter for a properly aligned femoral component **104** relative to a properly aligned acetabular component **103** to together define a properly aligned endoprosthetic hip implant **102**. A third alignment parameter for the femoral stem **115** is the vertical position of the artificial femoral head **113** relative to the natural femoral head (see **126**) of the operative hip prior to resection.

[0063] **FIG. 4** depicts a misaligned acetabular component **103** relative to the reamed acetabulum **111** and a femoral component **104** that is too short for the reamed femoral canal (also known as the intramedullary bore **119**). As shown, the abduction angle **α** and the anteversion angle **υ** are excessive. When the patient moves his or her hip during normal use, the neck **116** may contact the rim **2** of the acetabular shell **106**. Collectively, the rim **2** and the neck **116** can become a fulcrum for a lever that can dislocate the artificial femoral head **113** from the acetabular component **103**. Additionally, even if the femoral component **104** does not dislocate from the acetabular component **103**, the force distribution of the femoral head **113** relative to the inner liner **107** may be overly concentrated in a relatively small area, thereby increasing wear and reducing the longevity of the implant **102**.

[0064] **FIG. 4** also depicts a femoral stem **115** that is improperly sized and aligned relative to the intramedullary bore **119**. Improper sizing can occur when the femoral reaming (also known as a "broaching") tool does not create an intramedullary bore **119** that is large enough to remove cancellous bone that is peripheral to the inner cortical wall **120** of the femur **105**. Over time, the femoral stem **115** will compress any intermediate cancellous bone between the side of the femoral stem **115** and the inner cortical wall **120**, which will cause the femoral stem to subside in the intramedullary bore **119** and to become misaligned relative to the proximal femur **105**. Variability in broach placement can also lead to a varus tilt in which the longitudinal axis of the femoral stem **115** is disposed at a varus angle relative to the anatomical (*i.e.*, central, or longitudinal) axis of the distal femur **105**. For example, it is common that the surgeon will contact the lateral cortical wall **120** of the intramedullary canal **119** above the desired location of the femoral stem **115**. The surgeon may stop reaming upon contacting the lateral cortical wall **120** of the intramedullary canal **119** thinking that the patient has a narrow intramedullary canal **119** that will only accommodate a small femoral stem **115**. In reality, the longitudinal axis of the femoral stem **115** is disposed at a varus angle relative to the anatomical axis of the distal femur **105**. This subsidence and misalignment can ultimately change the length of one of the patient's legs relative to the other leg, which in turn alters the patient's gait. A halting gait changes the force distribution through the patient's body, which can further accelerate the wear of the endoprosthetic hip implant **102** as well as the wear of healthy cartilage **123** on the remaining natural hip joint **101b**.

[0065] Subsidence and misalignment of the femoral component **104** relative to the distal femur **105** can be especially difficult to achieve and to check with traditional 2D radiographs. This is because the femoral component **104** is inserted into the proximal femur **105** through the six to eight inch main incision. The surgeon's view of insertion is limited by the minimally invasive nature of the procedure and the femoral component is no longer visible to the unassisted eye once it enters the intramedullary bore **119**. Traditional 2D intraoperative radiographs (such a fluoroscopic images) do not show the third dimension, and therefore cannot provide an accurate real world depiction of the operative area **170** in 3D space.

[0066] Patient comfort and implant longevity are thought to depend in part on the placement and sizing of the artificial hip implant **102**. In general, the more closely the placement of a properly sized implant replicates the natural kinematics of the pre-diseased joint, the longer the implant can be expected to last and the more comfort the patient can be expected to experience.

[0067] In recent years, it has become possible to use 2D images, such as X-ray radiographs, to create 3D models of an operative area. These models can be used preoperatively to plan surgeries much closer to the date of the actual surgery. These models can also be used intraoperatively (*e.g.*, when projected on a display or across a surgeon's field of view).

[0068] However, X-ray radiographs have typically not been used as inputs for 3D models previously because of concerns about image resolution and accuracy. X-ray radiographs are 2D representations of 3D space. As such, a 2D X-ray radiograph necessarily distorts the image subject relative to the actual object that exists in three dimensions. Furthermore, the object through which the X-ray passes can deflect the path of the X-ray as it travels from the X-ray source **21** (typically the anode of the X-ray machine; see **FIG. 12**) to the X-ray detector **33** (which may include by non-limiting example, X-ray image intensifiers, phosphorus materials, flat panel detectors "FPD" (including indirect conversion FPDs and direct conversion FPDs), or any number of digital or analog X-ray sensors or X-ray film; see **FIG. 12**). Defects in the X-ray machine (see **1800**, **FIG. 12**) itself or in its calibration can also undermine the usefulness of X-ray photogrammetry and 3D model reconstruction. Additionally, emitted X-ray photons have different energies. As the X-rays interact with the matter placed between the X-ray source **21** and the detector **33**, noise and artifacts can be produced in part because of Compton and Rayleigh scattering, the photoelectric effect, extrinsic variables in the environment or intrinsic variables in the X-ray generation unit, X-ray detector, and/or processing units or displays.

[0069] Moreover, in a single 2D image, the 3D data of the actual subject is lost. As such, there is no data that a computational machine **1600** (*e.g.*, a computer) can use from a single 2D image to reconstruct a 3D model of the actual 3D object. For this reason, CT scans, MRIs, and other imaging technologies that preserve third dimensional data were often preferred inputs for reconstructing models of one or more subject orthopedic elements (*i.e.*, reconstructing a 3D model from actual 3D data generally resulted in more accurate, higher resolution models). However, certain exemplary embodiments of the present disclosure that are discussed below overcome these issues by using deep learning networks to improve the accuracy of reconstructed 3D models generated from X-ray input images.

[0070] There are a variety of methods to generate a 3D model from 2D preoperative or intraoperative images. By way of example, one such method may comprise receiving a set of 2D radiographic images of an operative area **170** of a patient with a radiographic imaging system, computing a first 3D model using epipolar geometry principles with a coordinate system of the radiographic imaging system and projective geometry data from the respective 2D images (see **FIGS. 8** and **9A**, **9B** and **9C**). Such an exemplary method may further comprise projecting the first 3D model on the 2D radiographic images and then adjusting the initial 3D model by registering the first and second radiographic images **30**, **50** on the first 3D model with an image-to-image registration technique. Once the image-to-image registration technique has been applied, a revised 3D model may be generated. This process can repeat until the desired clarity in achieved.

[0071] By way of another example, a deep learning network (also known as a "deep neural network" ("DNN"), such as a convolutional neural network ("CNN"), recurrent neural network ("RNN"), modular neural network, or sequence to sequence model, can be used to generate a 3D model of the subject orthopedic element (*i.e.*, a modeled orthopedic element **100b**) from a set of at least two 2D images of an operative area **170** of a patient. The 2D input images **30**, **50**, *etc.* are desirably tissue-penetrating images, such as radiographic images (*e.g.*, X-ray or fluoroscopy images). In such a method, the deep learning network can generate a model from the projective geometry data (*i.e.*, spatial data **43** or volume data **75**) from the respective 2D images. The deep learning network can have the advantage of being able to generate a mask of the different subject orthopedic elements **100** (*e.g.*, bones, soft tissues, *etc.*) in the operative area **170** as well as being able to calculate a volume (see **61** , **FIG. 7**) of one or more imaged orthopedic elements **100**. In exemplary embodiments, the dimensions of the identified orthopedic element **100** or of the component of an endoprosthetic implant assembly **102** can be mapped to spatial data **43** (**FIG. 8**) that is derived from the input images **30**, **50** (**FIG. 8**) to ascertain the position of the identified orthopedic element **100** or the component of the endoprosthetic implant assembly in 3D space. In this manner, the positions of the identified orthopedic element **100** and of the component of the endoprosthetic implant (*e.g.*, an acetabular component **104** or a femoral component **103**) can be ascertained relative to each other. If this information is displayed to the surgeon and is updated in real time or near real time based upon the surgeon's repositioning of the implant component relative to the identified orthopedic element, the surgeon can use exemplary embodiments in accordance with this disclosure to accurately align the implant component relative to the identified orthopedic element in three dimensions, while bypassing the limited field of view offered by the main incision.

[0072] It is contemplated that once the system is calibrated as discussed below, new tissue-penetrating images (*i.e.*, less than the number of input images needed to calibrate the system) can be taken intraoperatively to update the reconstructed model of the operative area (*e.g.*, to refresh the position of the identified component of the endoprosthetic implant related to another component of an endoprosthetic implant or relative to an identified orthopedic element). In other exemplary embodiments, the same number of new tissue-penetrating images as the number of input images chosen to calibrate the system can be used to refresh the position of the component of the endoprosthetic implant relative to another component of an endoprosthetic implant, or relative to and identified orthopedic element in the system.

[0073] **FIG. 5** is a flow chart outlining the steps of an exemplary method for ascertaining a position of an orthopedic element in space. The method comprises: step **1a** calibrating a tissue-penetrating machine, such as a radiographic imaging machine **1800** to determine a mapping relationship between image points (*e.g.*, X_L, X_R; **FIG. 8**) and corresponding space coordinates (*e.g.*,

x and *y* coordinates; **FIG. 8**) to define spatial data **43**, step **2a** capturing a first image **30** (**FIG. 8**) of an orthopedic element **100** using a radiographic imaging technique, wherein the first image **30** defines a first reference frame **30a**, step **3a** capturing a second image **50** (**FIG. 8**) of the orthopedic element **100** using the radiographic imaging technique, wherein the second image **50** defines a second reference frame **50a**, and wherein the first reference frame **30a** is offset from the second reference frame **50a** at an offset angle **θ**, step **4a** using a deep learning network to detect the orthopedic element using the spatial data **43**, the spatial data **43** defining anatomical landmarks on or in the orthopedic element **100**, the detected orthopedic element defining an identified orthopedic element **100a**, step **5a** using the deep learning network to apply a mask to the identified orthopedic element **100a** defined by an anatomical landmark, step **6a** projecting the spatial data **43** from the first image **30** of the identified orthopedic element **100a** and the spatial data **43** from the second image **50** of the identified orthopedic element **100a** to define volume data **75** (**FIG. 7**), wherein the spatial data **43** comprising image points (*e.g.*, X_L, X_R) disposed within a masked area of either the first image **30** or the second image **50** have a first value and wherein the spatial data **43** comprising image points (*e.g.*, X_L, X_R) disposed outside of a masked area of either the first image **30** or the second image **50** have a second value, wherein the first value is different from the second value, step **7a** applying the deep learning network to the volume data **75** to generate a reconstructed 3D model of the orthopedic element, to define a modeled orthopedic element **100b**; and step **8a** mapping the 3D modeled orthopedic element **100b** to the spatial data **43**. In other exemplary embodiments, step **4a** can comprise detecting the spatial data **43** defining anatomical landmarks on or in the orthopedic element **100** using a deep learning network.

[0074] **FIG. 6** is a flow chart outlining the steps of another exemplary method for ascertaining a position of an orthopedic element in space. The method comprises: step **1b** calibrating a tissue-penetrating imaging machine, such as a radiographic imaging machine to determine a mapping relationship between image points (*e.g.*, X_L, X_R) and corresponding space coordinates (*e.g.*, *x* and *y* coordinates) to define spatial data **43**, step **2b** capturing a first image **30** of an orthopedic element **100** using a radiographic imaging technique, wherein the first image **30** defines a first reference frame **30a**, step **3b** capturing a second image **50** of the orthopedic element **100** using the radiographic imaging technique, wherein the second image **50** defines a second reference frame **50a**, and wherein the first reference frame **30a** is offset from the second reference frame **50a** at an offset angle **θ**, step **4b** using a deep learning network to detect the orthopedic element **100** using the spatial data **43** to define an identified orthopedic element **100a**, the spatial data **43** defining anatomical landmarks on or in the orthopedic element **100**, step **5b** using the deep learning network to apply a mask to the identified orthopedic element **100a** defined by an anatomical landmark, step **6b** projecting the spatial data **43** from the first image **30** of the identified

orthopedic element **100a** and the spatial data **43** from the second image **50** of the identified orthopedic element **100a** to define volume data **75**, wherein the spatial data **43** comprising image points (*e.g.*, X_L, X_R) disposed within a masked area of either the first image **30** or the second image **50** have a first value and wherein the spatial data **43** comprising image points (*e.g.*, X_L, X_R) disposed outside of a masked area of the either the first image **30** or the second image **50** have a second value, wherein the first value is different from the second value, step **7b** applying the deep learning network to the volume data **75** to generate a reconstructed 3D model of the orthopedic element to define a modeled orthopedic element **100b**; and step **8b** mapping the modeled orthopedic element **100b** to the spatial data **43**, wherein the orthopedic element is a reamed acetabulum **111** of a pelvis **110**. In other exemplary embodiments, step **4b** can comprise detecting the spatial data **43** defining anatomical landmarks on or in the identified orthopedic element **100a** using a deep learning network.

[0075] It will be appreciated that in certain exemplary embodiments, the deep learning network can be the same deep learning network that has been separately trained to perform the discrete tasks (*e.g.*, identification of the orthopedic element **100** to define an identified orthopedic element **100a**, applying a mask to the identified orthopedic element **100a**, modeling the identified orthopedic element **100a** to define a modeled orthopedic element **100b**, *etc.*). In other exemplary embodiments, a different deep learning network can be used to perform one or more of the discrete tasks.

[0076] It is contemplated that exemplary methods and systems in accordance with this disclosure may be used in connection with a total hip arthroplasty ("THA"). In such exemplary embodiments, the orthopedic element **100** can be a femur **105**, femoral head **126**, pelvis **110**, acetabular cavity of the pelvis (*e.g.*, a natural acetabulum **108** or a reamed acetabulum **111**), and other boney anatomical landmark present in or near the operative area **170**. However, it will be appreciated that nothing in this disclosure limits the application of the exemplary systems and methods to use in a THA procedure. It is contemplated that exemplary systems and methods can be useful in any surgical procedure in which the presence of a significant amount of tissue obscures the view of the orthopedic element **100** or of the operative area **170** generally. Surgeries involving the shoulder, knee, or spine can be prime examples. Pediatric cardiothoracic procedures can be another example. Systems and methods in accordance with the present disclosure can further be useful with wrist and ankle procedures even though the surgeon's visual field is generally less obscured by surrounding tissue than in shoulder, hip, and spinal procedures.

[0077] The above examples are provided for illustrative purposes and are in no way intended to limit the scope of this disclosure. All methods for generating a 3D model from 2D

radiographic images of the same subject taken from at least two transverse positions are considered to be within the scope of this disclosure.

[0078] **FIGs. 7** and **8** illustrate how the first input image **30** and the second input image **50** can be combined to create a volume **61** comprising volume data **75** (**FIG. 7**). In **FIG.7**, the imaged operative area **170** is of a knee joint. **FIG. 7** provides an example of how a deep learning network can take volume data **75** from two calibrated input images **30** , **50** that are offset from one another by an offset angle **θ**, can generate one or more modeled orthopedic elements **100b** from the volume data **75**. In **FIG. 7**, the operative area **170** is that of a knee joint.

[0079] **FIG. 8** illustrates basic principles of epipolar geometry than can be used to convert spatial data **43** from the respective input images **30**, **50** into volume data **75**. It will be appreciated that the spatial data **43** is defined by a collection of image points (*e.g.*, X_L, X_R) mapped to corresponding space coordinates (*e.g.*, *x* and *y* coordinates) for a given input image **30**, **50**.

[0080] **FIG. 8** is a simplified schematic representation of a perspective projection described by the pinhole camera model. **FIG. 8** conveys basic concepts related to computer stereo vison, but it is by no means the only method by which 3D models can be reconstructed from 2D stereo images. In this simplified model, rays emanate from the optical center (*i.e.*, the point within a lens at which the rays of electromagnetic radiation (*e.g.*, visible light, X-rays, etc.) from the subject object are assumed to cross within the imaging machine's sensor or detector array **33** (**FIG. 12**). The optical centers are represented by points O_L, O_R in **FIG. 8**. In reality, the image plane (see **30a**, **50a**) is usually behind the optical center (*e.g.*, O_L, O_R) and the actual optical center is projected onto the detector array **33** as a point, but virtual image planes (*see* **30a**, **50a**) are presented here for illustrating the principles more simply.

[0081] The first input image **30** is taken from a first reference frame **30a**, while the second input image **50** is taken from a second reference frame **50a** that is different from the first reference frame **30a**. Each image comprises a matrix of pixel values. The first and second reference frames **30a**, **50a** are desirably offset from one another by an offset angle **θ**. The offset angle **θ** can represent the angle between the *x*-axis of the first reference frame **30a** relative to the *x*-axis of the second reference frame **50a**. Stated differently, the angle between the orientation of the orthopedic element in the first image and the orthopedic element in the second image can be known as the "offset angle."

[0082] Point e_L is the location of the second input image's optical center O_R on the first input image **30**. Point e_R is the location of the first input image's optical center O_L on the second input image **50**. Points e_L and e_R are known as "epipoles" or epipolar points and lie on line $O_L - O_R$. The points X, O_L, O_R define an epipolar plane.

[0083] Because the actual optical center is the assumed point at which incoming rays of electromagnetic radiation from the subject object cross within the detector lens, in this model, the rays of electromagnetic radiation can actually be imagined to emanate from the optical centers O_L, O_R for the purpose of visualizing how the position of a 3D point **X** in 3D space can be ascertained from two or more input images **30**, **50** captured from a detector **33** of known relative position. If each point (*e.g.*, X_L) of the first input image **30** corresponds to a line in 3D space, then if a corresponding point (*e.g.*, X_R) can be found in the second input image, then these corresponding points (*e.g.*, X_L, X_R) must be the projection of a common 3D point X. Therefore, the lines generated by the corresponding image points (*e.g.*, X_L, X_R) must intersect at 3D point X. In general, if the value of X is calculated for every corresponding image points (*e.g.*, X_L, X_R) in two or more input images **30**, **50**, a 3D volume **61** comprising volume data **75** can be reproduced from the two or more input images **30**, **50**. The value of any given 3D point X can be triangulated in a variety of ways. A non-limiting list of example calculation methods include the mid-point method, the direct linear transformation method, the essential matrix method, the line—line intersection method, and the bundle adjustment method. Furthermore, in certain exemplary embodiments, a deep learning network can be trained on a set of input images to establish a model for determining the position of a given point in 3D space based upon two or more input images of the same subject, wherein the first input image **30** is offset from the second input image **50** at an offset angle **θ**. It will further be appreciated that combinations of any of the above methods are within the scope of this disclosure.

[0084] It will be appreciated that "image points" (*e.g.*, X_L, X_R) described herein may refer to a point in space, a pixel, a portion of a pixel, or a collection of adjacent pixels. It will also be appreciated that 3D point **X** as used herein can represent a point in 3D space. In certain exemplary applications, 3D point **X** may be expressed as a voxel, a portion of a voxel, or a collection of adjacent voxels.

[0085] However, before principles of epipolar geometry can be applied, the position of each image detector **33** relative to the other image detector(s) **33** should be determined (or the position of a sole image detector **33** must be determined at the point in time in which the first image **30** was taken and the adjusted position of the sole image detector **33** should be known at the point in time in which the second image **50** was taken). It can also be desirable to determine the focal length and the optical center of the imaging machine **1800**. To ascertain this practically, the image detector **33** (or image detectors) is/are first calibrated. **FIGS. 9A**, **9B**, and **9C** depict calibration jigs **973A**, **973B**, **973C** relative to subject orthopedic elements **100**. In these figures, the example orthopedic elements **100** include are the proximal aspect of the femur **105** and the natural acetabulum **108** of the pelvis **110** that comprises a hip joint **101**.

[0086] Although at least two input images **30**, **50** are technically required for calibrating the exemplary systems described herein, at least three input images **30**, **50**, **70** can be desirable when the input images are radiographic input images and wherein the target operative area **170** involves a contralateral joint that cannot be easily isolated from radiographic imaging. For example, the pelvis **110** comprises contralateral acetabula **108**. A direct medial-lateral radiograph of the pelvis **110** would show both the acetabulum that is proximal to the detector **33** and the acetabulum that is distal to the detector **33**. However, because of the positioning of the pelvis **110** relative to the detector **33** and because a single 2D radiograph lacks 3D data, the relative acetabula will appear superimposed upon one another and it would be difficult for a person or a computational machine **1600** to distinguish which is the proximal and which is the distal acetabulum.

[0087] To address this issue, at least three input images **30**, **50**, **70** can be used. In one exemplary embodiment, the first input image **30** can be a radiograph that captures an anterior-posterior perspective of the operative area **170** (*i.e.*, an example of a first reference frame **30a**). For the second input image **50**, the patient or the detector **33** can be rotated clockwise (which can be designated by a positive degree) or counterclockwise (which can be designated by a negative degree) relative to the patient's orientation for the first input image **30**. For example, for the second input image **50**, the patient may be rotated plus or minus 45° from the patient's orientation in the first input image **30**. Likewise, the patient may be rotated clockwise or counterclockwise relative to the patient's orientation for the first input image **30**. For example, for the third input image **70**, the patient may be rotated plus or minus 45° relative to the patient's orientation in the first input image **30**. It will be appreciated that if the second input image **50** has a positive offset angle (*e.g.*, + 45°) relative to the orientation of the first input image **30**, the third input angle **70** desirably has a negative offset angle (*e.g.*, - 45°) relative to the orientation of the first input image **30** and vice versa.

[0088] In exemplary embodiments, the principles or epipolar geometry can be applied to at least three input images **30**, **50**, **70** taken from at least three different reference frames **30a**, **50a**, **70a** to calibrate exemplary systems.

[0089] **FIG. 9A** is an anterior-posterior view of the example orthopedic elements **100** (*e.g.*, a proximal femur **105**, a natural acetabulum **108**, a pelvis **110**, articular cartilage, other soft tissue, *etc.*) in an example operative area **170**. That is, **FIG. 9A** represents a first image **30** taken from a first reference frame **30a** (*e.g.*, a first transverse position). A first calibration jig **973A** is attached to a first holding assembly **974A**. The first holding assembly **974A** may comprise a first padded support **971A** engaged to a first strap **977A**. The first padded support **971A** is attached externally to the patient's thigh via the first strap **977A**. The first holding assembly **974A** supports the first calibration jig **973A** that is oriented desirably parallel to the first reference frame **30a** (*i.e.*,

orthogonal to the detector **33**). The calibration jig **973A** is desirably positioned sufficiently far away from the desired subject orthopedic elements **100** such that the calibration jig **973A** do not overlap any subject orthopedic element **100**. Overlapping my obscure desirable image data.

[0090] **FIG. 9B** is a view of the example orthopedic elements **100** (*e.g.*, a proximal femur **105**, a natural acetabulum **108**, a pelvis **110**, articular cartilage, other soft tissue, *etc.*) of the example operative area **170** of **FIG. 9A** that is positively offset from the first reference frame **30a** by 45°. That is, **FIG. 9B** represents a second input image **50** taken from a second reference frame **50a** (*e.g.*, a second transverse position). A second calibration jig **973B** is attached to the second holding assembly **974B**. The second holding assembly **974B** may comprise a second padded support **971B** engaged to a second strap **977B**. The second padded support **971B** is attached externally to the patient's thigh via the second strap **977B**. The second holding assembly **974B** supports the second calibration jig **973B** that is oriented desirably parallel to the second reference frame **50a** (*i.e.*, orthogonal to the detector **33**). The calibration jig **973B** is desirably positioned sufficiently far away from the subject orthopedic elements **100** such that the calibration jig **973B** does not overlap any subject orthopedic element **100**.

[0091] **FIG. 9C** is a view of the example orthopedic elements **100** (*e.g.*, a proximal femur **105**, a natural acetabulum **108**, a pelvis **110**, articular cartilage, other soft tissue, *etc.*) of the example operative area **170** of **FIG. 9A** that is negatively offset from the first reference frame **30a** by 45°. That is, **FIG. 9C** represents a third input image **70** taken from a third reference frame **70a** (*e.g.*, a third transverse position). A third calibration jig **973C** is attached to the third holding assembly **974C**. The third holding assembly **974C** may comprise a third padded support **971C** engaged to a third strap **977C**. The third padded support **971C** is attached externally to the patient's thigh via the third strap **977C**. The third holding assembly **974C** supports the third calibration jig **973C** that is oriented desirably parallel to the third reference frame **70a** (*i.e.*, orthogonal to the detector **33**). The calibration jig **973C** is desirably positioned sufficiently far away from the subject orthopedic elements **100** such that the calibration jig **973C** does not overlap any subject orthopedic element **100**.

[0092] If the system is calibrated preoperatively, the patient may be posited in the standing position (*i.e.*, the leg is in extension) because the hip joint is stable in this orientation (see **FIG. 12**). If the system in calibrated intraoperatively, the patient may be lying supine on the operating table. Preferably, the patient's distance relative to the imaging machine should not be altered during the acquisition of the input images **30**, **50**, **70**. The first, second, and third input images **30**, **50**, **70** need not capture the entire leg, rather the image can focus on the joint that will be the subject of the operative area **170**.

[0093] It will be appreciated that depending upon the subject orthopedic elements **100** to be imaged and modeled, only a single calibration jig **973** may be used. Likewise, if a particularly long collection of orthopedic elements **100** are to be imaged and modeled, more than one calibration jigs **973** may be used.

[0094] Each calibration jig **973A**, **973B**, **973C** is desirably of a known size. Each calibration jig **973A**, **973B**, **973C** desirably has at least four or more calibration points **978** distributed throughout. The calibration points **978** are distributed in a known pattern in which the distance from one point **978** relative to the others is known. The distance from the calibration jig **973** from an orthopedic element **100** can also desirably be known. For calibration of an X-ray photogrammetry system, the calibration points **978** may desirably be defined by metal structures on the calibration jig **973**. Metal typically absorbs most X-ray beams that contact the metal. As such, metal typically appears very brightly relative to material that absorbs less of the X-rays (such as air cavities or adipose tissue). Common example structures that define calibration points include, but are not limited to: *reseau* crosses, circles, triangles, pyramids, and spheres.

[0095] These calibration points **978** can exist on a 2D surface of the calibration jig **973**, or 3D calibration points **978** can be captured as 2D projections from a given image reference frame. In either situation, the 3D coordinate (commonly designated the z coordinate) can be set to equal zero for all calibration points **978** captured in the image. The distance between each calibration point **978** is known. These known distances can be expressed as x, y coordinates on the image sensor/detector **33**. To map a point in 3D space to a 2D coordinate pixel on a sensor **33**, the dot product of the detector's calibration matrix, the extrinsic matrix and the homologous coordinate vector of the real 3D point can be used. This permits the real world coordinates of a point in 3D space to be mapped relative to calibration jig **973**. Stated differently, this generally permits the x, y coordinates of the real point in 3D space to be transformed accurately to the 2D coordinate plane of the image detector's sensor **33** to define spatial data **43** (see **FIG. 8**).

[0096] The above calibration method is provided as an example. It will be appreciated that all methods suitable for calibrating an X-ray photogrammetry system are considered to be within the scope of this disclosure. A non-limiting list of other X-ray photogrammetry system calibration methods include the use of a *reseau* plate, the Zhang method, the bundle adjustment method, direct linear transformation methods, maximum likelihood estimation, a k-nearest neighbor regression approach ("KNN"), a convolutional neural network ("CNN") based approach, other deep learning methods, or combinations thereof.

[0097] **FIG. 7** illustrates the principle of how two calibrated input images **30**, **50**, when oriented along the known offset angle **θ**, can be back projected into a 3D volume **61** comprising two channels **65**, and **66**. The first channel **65** contains all the image points (*e.g.*, X_L *etc.*) of the first

input image **30** and the second channel **66** contains all the image points (*e.g.*, X_R *etc.*) of the second input image **50**. That is, each image point (*e.g.*, pixel) is replicated over its associated back-projected 3D ray. Next, epipolar geometry can be used to generate a volume **61** of the imaged operative area **170** comprising volume data **75** from these back projected 2D input images **30**, **50**. If a third input image **70** is used, a third channel containing all of the image points of the third input image **70** can be present.

[0098] Referring to **FIG. 7**, the first input image **30** and the second input image **50** desirably have known image dimensions. The dimensions may be pixels. For example, the first image **30** may have dimensions of 164 x 164 pixels. The second image **50** may have dimensions of 164 x 164 pixels. The dimensions of the input images **30**, **50** used in a particular computation desirably have consistent dimensions. Consistent dimensions may be desirable for later defining a cubic working area of regular volume **61** (*e.g.*, a 164 x 164 x 164 cube). In embodiments, the offset angle **θ** is desirably 45° between each adjacent input image. However, other offset angles **θ** may be used in other exemplary embodiments. For example, in **FIG. 7**, the offset angle **θ** is 90°.

[0099] In the depicted example, each of the 164 x 164 pixel input images **30**, **50** are replicated 164 times over the length of the adjacent input image to create a volume **61** having dimensions of 164 x 164 x 164 pixels. That is, the first image **30** is copied and stacked behind itself at one copy per pixel for 164 pixels while the second image **50** is copied and stacked behind itself for 164 pixels such that stacked images overlap to thereby create the volume **61**. In this manner, the volume **61** can be said to comprise two channels **65**, **66**, wherein the first channel **65** comprises the first image **30** replicated *n* times over the length of the second image **50** (*i.e.*, the *x*-axis of the second image **50**) and the second channel **66** comprises the second image **50** replicated *m* times over the length of the first image **30** (*i.e.*, the *x*-axis of the first image **30**), wherein "*n*" and "*m*" are the length of the indicated image as expressed as the number of pixels (or other dimensions on other exemplary embodiments) that comprise the length of the indicated image. If the offset angle **θ** is known, each transverse slice (also known as an "axial slice" by some radiologists) of the volume **61** creates an epipolar plane comprising voxels that are back projected from the pixels that comprise the two epipolar lines. In this manner, projecting spatial data **43** from the first image **30** of the subject orthopedic element **100** and the spatial data **43** from the second image **50** of the subject orthopedic element **100** defines the volume data **75**. Using this volume data **75**, the 3D representation can be reconstructed using epipolar geometric principles as discussed above; the 3D representation is consistent geometrically with the information in the input images **30**, **50**.

[00100] In exemplary systems and methods for identifying an orthopedic element and/or a component of an endoprosthetic implant and in exemplary systems and methods for ascertaining a position of an orthopedic element and a component of an endoprosthetic implant in space using a

deep learning network, wherein the deep learning network is a CNN, a detailed example of how the CNN can be structured and trained is provided. All architecture of CNNs are considered to be within the scope of this disclosure. Common CNN architectures include by way of example, LeNet, GoogLeNet, AlexNet, ZFNet, ResNet, and VGGNet.

[00101] Preferably, the methods disclosed herein may be implemented on a computer platform (see **1600**) having hardware such as one or more central processing units (CPU), a random access memory (RAM), and input/output (I/O) interface(s).

[00102] **FIG. 10** is a schematic representation of a CNN that illustrates how the CNN can be used to identify the edges of a subject orthopedic element **100**. Without being bound by theory, it is contemplated that a CNN may be desirable for reducing the size of the volume data **75** without losing features that are necessary to identify the desired orthopedic element **100** or its surface topography. The volume data **75** of the multiple back projected input images **30**, **50** is a multidimensional array that can be known as an "input tensor." This input tensor comprises the input data (which is the volume data **75** in this example) for the first convolution. A filter (also known as a kernel **69**) is shown disposed in the volume data **75**. The kernel **69** is a tensor (*i.e.*, a multi-dimensional array) that defines a filter or function (this filter or function is sometimes known as the "weight" given to the kernel). In the depicted embodiment, the kernel tensor **69** is three dimensional. The filter or function that comprises the kernel **69** can be programed manually or learned through the CNN, RNN, or other deep learning network. In the depicted embodiment, the kernel **69** is a 3x3x3 tensor although all tensor sizes and dimensions are considered to be within the scope of this disclosure, provided that the kernel tensor size is less than the size of the input tensor.

[00103] Each cell or voxel of the kernel **69** has a numerical value. These values define the filter or function of the kernel **69**. A convolution or cross-correlation operation is performed between the two tensors. In **FIG. 10**, the convolution is represented by the path **76**. The path **76** that the kernel **69** follows is a visualization of the mathematical convolution operation. Following this path **76**, the kernel **69** eventually and sequentially traverses the entire volume **61** of the input tensor (*e.g.*, the volume data **75**). The goal of this operation is to extract features from the input tensor.

[00104] Convolution layers **72** typically comprise one or more of the following operations: a convolution stage **67**, a detector stage **68**, and a pooling stage **58**. Although these respective operations are represented visually in the first convolution layer **72a** in **FIG. 10**, it will be appreciated that the subsequent convolution layers **72b**, **72c**, *etc.* may also comprise one or more or all of the convolution stage **67**, detector stage **68**, and pooling layer **58** operations or combinations or permutations thereof. Furthermore, although **FIG. 10**, depicts five convolution

layers **72a**, **72b**, **72c**, **72d**, **72e** of various resolutions, it will be appreciated that more or less convolution layers may be used in other exemplary embodiments.

[00105] In the convolution stage **67**, the kernel **69** is sequentially multiplied by multiple patches of pixels in the input data (*i.e.*, the volume data **75** in the depicted example). The patch of pixels extracted from the data is known as the receptive field. The multiplication of the kernel **69** and the receptive field comprises an element-wise multiplication between each pixel of the receptive field and the kernel **69**. After multiplication, the results are summed to form one element of a convolution output. This kernel **69** then shifts to the adjacent receptive field and the element-wise multiplication operation and summation continue until all the pixels of the input tensor have been subjected to the operation.

[00106] Until this stage, the input data (*e.g.*, the volume data **75**) of the input tensor has been linear. To introduce non-linearity to this data, a nonlinear activation function is then employed. Use of such a non-linear function marks the beginning of the detector stage **68**. A common non-linear activation function is the Rectified Linear Unit function ("ReLU"), which is given by the function:

[00107] $ReLU(x) = \begin{cases} 0, if\ x < 0 \\ x, if\ x \geq 0 \end{cases}$

[00108] When used with bias, the non-linear activation function serves as a threshold for detecting the presence of the feature extracted by the kernel **69**. For example, applying a convolution or a cross-correlation operation between the input tensor and the kernel **69**, wherein the kernel **69** comprises a low level edge filter in the convolution stage **67** produces a convolution output tensor. Then, applying a non-linear activation function with a bias to the convolution output tensor will return a feature map output tensor. The bias is sequentially added to each cell of the convolution output tensor. For a given cell, if the sum is greater than or equal to 0 (assuming ReLU is used in this example), then the sum will be returned in the corresponding cell of the feature map output tensor. Likewise, if the sum is less than 0 for a given cell, then the corresponding cell of the feature map output tensor will be set to 0. Therefore, applying non-linear activation functions to the convolution output behaves like a threshold for determining whether and how closely the convolution output matches the given filter of the kernel **69**. In this manner, the non-linear activation function detects the presence of the desired features from the input data (*e.g.*, the volume data **75** in this example).

[00109] All non-linear activation functions are considered to be within the scope of this disclosure. Other examples include the Sigmoid, TanH, Leaky ReLU, parametric ReLU, Softmax, and Switch activation functions.

[00110] However, a shortcoming of this approach is that the feature map output of this first convolutional layer **72a** records the precise position of the desired feature (in the above example, an edge). As such, small movements of the feature in the input data will result in a different feature map. To address this problem and to reduce computational power, down sampling is used to lower the resolution of the input data while still preserving the significant structural elements. Down sampling can be achieved by changing the stride of the convolution along the input tensor. Down sampling is also achieved by using a pooling layer **58**.

[00111] Valid padding may be applied to reduce the dimensions of the convolved tensor (see **72b**) compared to the input tensor (see **72a**). A pooling layer **58** is desirably applied to reduce the spatial size of the convolved data, which decreases the computational power required to process the data. Common pooling techniques, including max pooling and average pooling may be used. Max pooling returns the maximum value of the portion of the input tensor covered by the kernel **69**, whereas average pooling returns the average of all the values of the portion of the input tensor covered by the kernel **69**. Max pooling can be used to reduce image noise.

[00112] In certain exemplary embodiments, a fully connected layer can be added after the final convolution layer **72e** to learn the non-linear combinations of the high level features (such as for example, the profile of an imaged natural acetabulum **108**, the profile of a reamed acetabulum **109**, or the surface topology of the orthopedic element) represented by the output of the convolutional layers.

[00113] When used on an orthopedic element **100**, the above description of a CNN type deep learning network is one example of how a deep learning network can be "configured to identify" an orthopedic element **100** to define an "identified orthopedic element" **100a**.

[00114] The top half of **FIG. 10** represents compression of the input volume data **75**, whereas the bottom half represents decompression until the original size of the input volume data **75** is reached. The output feature map of each convolution layer **72a** , **72b**, **72c**, *etc.* is used as the input for the following convolution layer **72b**, **72c**, *etc.* to enable progressively more complex feature extraction. For example, the first kernel **69** may detect edges, a kernel in the first convolution layer **72b** may detect a collection of edges in a desired orientation, a kernel in a third convolution layer **72c** may detect a longer collection of edges in a desired orientation, *etc.* This process may continue until the entire profile of the desired orthopedic element **100** is detected and identified by a downstream convolution layer **72**.

[00115] The bottom half of **FIG. 10** up-samples (*i.e.*, expands the spatial support of the lower resolution feature maps. A de-convolution operation is performed in order to increase the size of the input for the next downstream convolutional layer (see **72c**, **72d**, **72e**). For the final convolution layer **72e**, a convolution can be employed with a 1 x 1 x 1 kernel **69** to produce a multi-

channel output volume **59** that is the same size as the input volume **61**. Each channel of the multi-channel output volume **59** can represent a desired extracted high level feature. This can be followed by a Softmax activation function to detect the desired orthopedic elements **100**. For example, the depicted embodiment may comprise five output channels numbered 0, 1, 2, 3, 4, wherein channel 0 represents identified background volume, channel 1 represents the identified proximal femur **105**, channel 2 represents the identified reamed acetabulum **111**, channel 3 represents the identified acetabular component **103**, and channel 4 represents the identified femoral component **104**.

[00116] It will be appreciated that less output channels or more output channels may be used in other exemplary embodiments. It will also be appreciated that the provided output channels may represent different orthopedic elements **100** and components of endoprosthetic implants than those listed here.

[00117] For example, in exemplary embodiments in which the system is configured to identify an orthopedic element **100**, wherein the orthopedic element **100** is the inner cortical wall **120** of the proximal femur **105** and in which the system is configured to identify a component of an endoprosthetic implant, wherein the component of the endoprosthetic implant is a trial component construct, the exemplary embodiment may comprise three output channels numbered 0, 1, 2, wherein channel 0 represents identified background volume, channel 1 represents the inner cortical wall **120** of the proximal femur **105**, and channel 2 represents the identified femoral component **104**. A "trial component construct" as used in the above example, when the trial component construct describes a construct to be used in the proximal femur **105** can include a broach, trial neck, and trial head assembly, or a trial stem.

[00118] In exemplary embodiments in which the system is configured to identify an orthopedic element **100**, wherein the orthopedic element **100** is the reamed acetabulum **111** of the pelvis **110** and in which the system is configured to identify a component of an endoprosthetic implant, wherein the component of the endoprosthetic implant is an acetabular component **103** or a trial acetabular component, the exemplary embodiment may comprise three output channels numbered 0, 1, 2, wherein channel 0 represents identified background volume, channel 1 represents the reamed acetabulum **111** of the pelvis **110**, and channel 2 represents the an acetabular component **103** or the trial acetabular component.

[00119] Such exemplary embodiments can optionally comprise additional output channels, such as an output channel that represents the outer wall of the proximal femur **105**. Other output channels can be used to output the abduction angle $\boldsymbol{\alpha}$ and the anteversion angle $\boldsymbol{\upsilon}$ respectively of the identified component of an endoprosthetic implant relative to the identified orthopedic element **100a** in which the component of the endoprosthetic implant sits. Still other output channels may be used to output (by way of non-limiting examples) a determined size dimension of the

identified orthopedic element, a recommended component type/product model of an endoprosthetic implant, a recommended component size of an endoprosthetic implant, a "best fit" output of a recommend component or of a recommended component size relative to the dimensions of the inner cortical wall **120**, an alignment calculation of the longitudinal axis of the femoral component **104**, a trial component construct relative to an anatomical axis of the proximal femur **105**, the calculated center of the acetabulum, or the alignment of a longitudinal axis of the neck of the femoral component **104** relative to the center of the artificial femoral head **113**. Combinations of any of the foregoing are considered to be within the scope of this disclosure.

[00120] When used on a component of an endoprosthetic implant or subcomponents thereof, the above description of a CNN type deep learning network is one example of how a deep learning network can be "configured to identify" a component of an endoprosthetic implant (or subcomponents thereof) to define an identified component of the endoprosthetic implant. When used on an endoprosthetic implant, the above description of a CNN type deep learning network is one example of how a deep learning network can be "configured to identify" an endoprosthetic implant to define an "identified endoprosthetic implant." It will be further understood that when applied to multiple orthopedic elements, multiple components of endoprosthetic implants, multiple endoprosthetic implants, or combinations thereof, the above description of a CNN type deep learning network is one example of how a deep learning network can be "configured to identify" multiple orthopedic elements, multiple components of endoprosthetic implants, subcomponents thereof, multiple endoprosthetic implants, or combinations thereof as the case may be. Other deep learning network architectures known or readily ascertainable by those having ordinary skill in the art are also considered to be within the scope of this disclosure.

[00121] In exemplary embodiments, select output channels comprising output volume data **59** of the desired orthopedic element **100** can be used to generate a modeled orthopedic element **100b**, a modeled component of an endoprosthetic implant (*e.g.*, an acetabular cup **106** , a femoral stem **115**, *etc.*). In certain exemplary embodiments, the modeled orthopedic element **100b** is a computer model. In other exemplary embodiments, the modeled orthopedic element **100b** is a physical model.

[00122] Although the above example described the use of a three dimensional tensor kernel **69** to convolve the input volume data **75**, it will be appreciated that the general model described above can be used with 2D spatial data **43** from any of the calibrated input images **30**, **50**, **70**. In other exemplary embodiments, a machine learning algorithm (*i.e.*, a deep learning network (such as for example, a CNN)) can be used after calibration of the imaging machine **1800** but before 2D to 3D reconstruction. That is, the CNN can be used to detect features (*e.g.*, anatomical landmarks) of a subject orthopedic element **100** from the first reference frame **30a**, the second

reference frame **50a**, or the third reference frame **70a** of the 2D input images **30**, **50**, **70**. In exemplary embodiments, a CNN may be used to identify high level orthopedic elements (*e.g.*, the proximal femur **105** and a portion of the surface topology of the subject orthopedic element **100**), components of an endoprosthetic implant (*e.g.*, the acetabular cup **106**, femoral stem **115**, *etc.*) or the endoprosthetic implant itself (*e.g.* the hip endoprosthetic implant **102**) from the 2D input images **30**, **50**, **70**. The CNN may then optionally apply a mask or an outline to the detected orthopedic element **100**, component of an endoprosthetic implant, or the endoprosthetic implant itself. It is contemplated that if the imaging machine **1800** is calibrated, and if the CNN identified multiple corresponding image points (*e.g.*, X_L, X_R) of features between the at least two input images **30**, **50**, then the transformation matrices between the reference frames **30a**, **50a** of a subject orthopedic element **100**, component of an endoprosthetic implant, or the endoprosthetic implant itself can be used to align the multiple corresponding image points in 3D space. In this manner, the position of the points in 3D space can be determined to correspond to a set of coordinates in 3D space. In this manner, the 3D points can be said to be "mapped" to spatial data. A deep learning network that is capable of modeling this relationship in this manner or in other manners developed by the deep learning network can be said to be "configured to map" the identified orthopedic element, the identified component of the endoprosthetic implant, and/or the endoprosthetic implant itself (as the case may be) to spatial data ascertained by the first input image **30** and the second input image **50** (and optionally the third input image **70** or further input images or 'new' refreshing images) to thereby determine the position of the identified orthopedic element **100a**, the identified component of the endoprosthetic implant, and/or the endoprosthetic implant itself (as the case may be) in three dimensional space.

[00123] In embodiments wherein any of the first input image **30**, the second input image **50**, or the third input image **70** are radiographic X-ray images (including, but not limited to fluoroscopic radiographic images), training a CNN can present several challenges. By way of comparison, CT scans typically produce a series of images of the desired volume. Each CT image that comprises a typical CT scan can be imagined as a segment of the imaged volume. From these segments, a 3D model can be created relatively easily by adding the area of the desired element as the element is depicted in each successive CT image. The modeled element can then be compared with the data in the CT scan to ensure accuracy. One drawback of CT scans is that CT scans expose the patient to excessive amounts of radiation (about seventy times the amount radiation of one traditional radiograph).

[00124] By contrast, radiographic imaging systems typically do not generate sequential images that capture different segments of the imaged volume; rather, all of the information of the image is flattened on the 2D plane. Additionally, because a single radiographic image **30** inherently

lacks 3D data, it is difficult to check the model generated by the epipolar geometry reconstruction technique described above with the actual geometry of the target orthopedic element **100**. To address this issue, the CNN can be trained with CT images, such as digitally reconstructed radiograph ("DRRs") images. By training the deep learning network in this way, the deep learning network can develop its own weights (*e.g.*, filters) for the kernels **69** to identify a desired orthopedic element **100** or surface topography of a subject orthopedic element **100**. Because X-ray radiographs have a different appearance than DRRs, image-to-image translation can be performed to render the input X-ray images to have a DRR-style appearance. An example image-to-image translation method is the Cycle-GAN image translation technique. In embodiments in which image-to-image style transfer methods are used, the style transfer method is desirably used prior to inputting the data into a deep learning network for feature detection.

[00125] The above examples are provided for illustrative purposes and are in no way intended to limit the scope of this disclosure. All methods for generating a 3D model of the subject orthopedic element **100** from 2D radiographic images of the same subject orthopedic element **100** taken from at least two transverse positions (*e.g.*, **30a**, **50a**) are considered to be within the scope of this disclosure.

[00126] Determining the metes and bounds of a particular identified orthopedic element **100a** component of the endoprosthetic implant, and/or the endoprosthetic implant, component of the endoprosthetic implant, and/or the endoprosthetic implant itself and their precise coordinates in 3D space, permits the position of the identified orthopedic element **100a**, component of the endoprosthetic implant, and or the endoprosthetic implant, component of the endoprosthetic implant, and or the endoprosthetic implant to be known while bypassing the limited field of view offered to the surgeon through the main incision. If the position of the identified orthopedic element **100a** is known, and if the position of the identified component of the endoprosthetic implant is known, then this information can be used to check against the desired alignment parameters of the implant component relative to the identified orthopedic element **100a** into which the implant component is installed (*e.g.* an acetabular shell **106** installed into a reamed acetabulum **111**, a femoral stem **115** installed into the intramedullary canal of the proximal femur **105**, *etc.*).

[00127] Likewise, if the position of a first component of an endoprosthetic implant (*e.g.*, the acetabular component) is known relative to a second component of the endoprosthetic implant (*e.g.*, the femoral component) in three dimensions, then the surgeon can use the exemplary systems and methods described herein to evaluate the placement and therefore the alignment of the first component relative to the second component. The surgeon may re-image the operative area to update the position of the first component relative to the second component at subsequent time intervals until the surgeon is satisfied with the alignment. It is contemplated that such alignment

may be performed intraoperatively to mitigate the problems of misaligned components of multi-component endoprosthetic implants.

[00128] In certain exemplary embodiments that comprise using a deep learning network to add a mask or an outline to the detected 2D orthopedic element **100** from the respective input images **30**, **50**, **70** only the 2D masks or outlines of the identified orthopedic element **100** component of the endoprosthetic implant, and/or the endoprosthetic implant can be sequentially back projected in the manner described with reference to **FIGs. 7** and **8** *supra* to define a volume **61** of the identified orthopedic element **100**, component of the endoprosthetic implant, and/or the endoprosthetic implant. In this exemplary manner, a modeled orthopedic element **100b**, modeled component of the endoprosthetic implant, and/or a modeled endoprosthetic implant may be generated.

[00129] **FIG. 11** is a close up of a modeled endoprosthetic implant **102b** comprising several modeled endoprosthetic implant components, namely, a modeled acetabular component **103b** and a modeled femoral component **104b**. The modeled acetabular component **103b** comprises a modeled acetabular shell **106b** and a modeled acetabular liner **107b**. The modeled femoral component **104b** comprises a modeled femoral stem **115b**, modeled femoral stem neck **116b**, and modeled artificial femoral head **113b**.

[00130] An exemplary system or method may further comprise calculating a center of the acetabulum. Such an exemplary system or method may still further comprise aligning a longitudinal rotational axis of a femoral stem implant with the center of the acetabulum. In still other exemplary systems or methods, the longitudinal axis of the femoral stem **115** can be aligned (*i.e.*, co-linear) with the longitudinal axis of the femur **105**. In still other exemplary systems and methods, the rotational axis of the neck of the femoral stem **115** can be aligned with the center of the artificial femoral head **113**. In still other exemplary systems and methods, the position of the artificial head **113** can be aligned (*e.g.*, vertically) with the pre-diseased natural femoral head based upon input images of the natural femoral head. In such exemplary embodiments, the longitudinal axis of the femoral stem **115** is desirably co-linear with the anatomical axis of the femur **105** and the femoral stem **115** is desirably disposed at an anteversion angle υ in the range of about 10° to about 30°, desirably about 15° to about 25°.

[00131] A computer platform, having hardware such as one or more central processing units (CPU), a random access memory (RAM), and input/output (I/O) interface(s) can receive at least two 2D radiographic images taken at different orientations along a transverse plane. The orientations can be orthogonal to each other (*i.e.,* the first reference frame has an offset angle θ of 90° relative to the second reference frame). However, in embodiments in which the orthopedic elements **100** comprise a hip joint **101**, at least three 2D radiographic input images can be desirable

to avoid interference from the contralateral acetabulum. In such exemplary embodiments, the offset angle **θ** can be desirably 45° among adjacent reference frames. Other obtuse or acute offset angles **θ** can be used in other exemplary embodiments.

[00132] Referring to **FIG. 12**, an exemplary system for ascertaining a position of an orthopedic element **100** and a component of an endoprosthetic implant in space can comprise: a tissue-penetrating imaging machine **1800** (such as a radiographic imaging machine, fluoroscopy machine, *etc.*) comprising an emitter **21** and a detector **33**, wherein the detector **33** of the radiographic imaging machine **1800** captures a first input image **30** (**FIGS. 8** and **9A**) in a first transversion position **30a** (**FIGS. 8** and **9A**) and a second input image **50** (**FIGS. 8** and **9B**) in a second transverse position **50a** (**FIGS. 8** and **9B**), wherein the first transverse position **30a** is offset from the second transverse position **50a** by an offset angle **θ** (**FIG. 8**). In exemplary embodiments involving at least three input images, the detector **33** of the radiographic imaging machine **1800** captures a third input image **70** (**FIGS. 8** and **9C**) in a third transverse position **70a** (**FIGS. 8** and **9C**), wherein the third transverse position **70a** is offset from the second transverse position **50a** and the first transverse position **30a** by two separate offset angles **θ1**, **θ2**.

[00133] The exemplary system can further comprise a transmitter **29** (**FIG. 12**), and a computational machine **1600** (see **FIG. 13** for further details) wherein the transmitter **29** transmits the first input image **30** and the second input image **50** (and optionally the third input image **70** if present) from the detector **33** to the computational machine **1600**, and wherein the computational machine **1600** is configured to identify an orthopedic element **100a**, component of an endoprosthetic implant, subcomponent of a component of an endoprosthetic implant, or the endoprosthetic implant itself using one of the deep learning methods discussed herein. It will be appreciated that the exemplary systems disclosed herein can be used pre-operatively, intraoperatively, and/or post operatively.

[00134] In certain exemplary embodiments, an exemplary system may further comprise a display **19**.

[00135] **FIG. 12** is a schematic representation of an exemplary system comprising a radiographic imaging machine **1800** comprising an X-ray source **21**, such as an X-ray tube, a filter **26**, a collimator **27**, and a detector **33**. In **FIG. 12**, the radiographic imaging machine **1800** is shown from the top down. The depicted radiographic imaging machine **1800** is a type of tissue-penetrating imaging machine. A patient **1** is disposed between the X-ray source **21** and the detector **33**. The radiographic imaging machine **1800** may be mounted on a rotatable gantry **28**. The radiographic imaging machine **1800** may take a first radiographic input image **30** of the patient **1** from a first reference frame **30a**. The gantry **28** may then rotate the radiographic imaging machine **1800** by an offset angle. The radiographic imaging machine **1800** may then take the second radiographic input

image **50** from the second reference frame **50a**. It will be appreciated that other exemplary embodiments can comprise using multiple input images taken at multiple offset angles **θ**. For example, in a hip arthroplasty, the radiographic imaging machine **1800** may be further rotated (or the patient rotated) to capture a third radiographic input images **70** from a third reference frame **70a**. In such embodiments, the offset angle may be less than or greater than 90° between adjacent input images.

[00136] It will be appreciated that the offset angle need not be exactly 90 degrees in every embodiment. An offset angle having a value within a range that is plus or minus 45 degrees is contemplated as being sufficient. In other exemplary embodiments, an operator may take more than two images of the orthopedic element using a radiographic imaging technique. It is contemplated that each subsequent image after the second image can define a subsequent image reference frame. For example, a third image can define a third reference frame, a fourth image can define a fourth reference frame, the n^{th} image can define an n^{th} reference frame, *etc.*

[00137] In other exemplary embodiments comprising three input images and three distinct reference frames, each of the three input images may have an offset angle **θ** of about 60 degrees relative to each other. In some exemplary embodiments comprising four input images and four distinct reference frames, the offset angle **θ** may be 45 degrees from an adjacent reference frame. In an exemplary embodiment comprising five input images and five distinct reference frames, the offset angle **θ** may be about 36 degrees from the adjacent reference frame. In exemplary embodiments comprising *n* images and *n* distinct reference frames, the offset angle **θ** can be 180/*n* degrees.

[00138] It is further contemplated that embodiments involving multiple images, especially more than two images do not necessarily have to have regular and consistent offset angles. For example, an exemplary embodiment involving four images and four distinct reference frames may have a first offset angle at 85 degrees, a second offset angle at 75 degrees, a third offset angle at 93 degrees, and a fourth offset angle at 107 degrees.

[00139] A transmitter **29** then transmits the first input image **30** and the second input image **50** to a computational machine **1600**. The computational machine **1600** can use a deep learning network to identify an orthopedic element **100a**, component of an endoprosthetic implant, subcomponent of a component of an endoprosthetic implant, or the endoprosthetic implant itself in any manner that is consistent with this disclosure.

[00140] **FIG. 12** also depicts another embodiment in which the output data from the computational machine **1600** is transmitted to a display **19**. A display **19** can depict a modeled endoprosthetic implant **102b**. The display may optionally display any of the items identified by the exemplary systems and methods described herein, including but not limited to the identified

endoprosthetic implant, component of the endoprosthetic implant or subcomponent thereof, or one or more orthopedic elements. In exemplary embodiments, it is contemplated that the identified component of the endoprosthetic implant, or the representative model of the component of the endoprosthetic implant can be superimposed on the identified orthopedic element into which the component of the endoprosthetic implant will be seated (*e.g.*, the femoral component and the proximal femur respectively). The superimposition can be calculated and displayed using the mapped spatial data of the respective identified elements (*e.g.*, the component of the endoprosthetic implant and the orthopedic element into which the component of the endoprosthetic implant will be seated).

[00141] In this manner, the surgeon and others in the operating room can have a near real time visualization of the component of the endoprosthetic implant and the target orthopedic element in three dimensions and their alignment relative to one another.

[00142] Furthermore, because the spatial data of an identified component of the endoprosthetic implant and because the spatial data of the identified orthopedic element can be obtained from exemplary systems described herein, the degree of alignment can be calculated and further displayed on a display **19** in exemplary system embodiments. For example, a calculated abduction angle **α** of the identified component of the endoprosthetic implant can displayed on a display. By way of another example, calculated anteversion angle **υ** of the identified component of the endoprosthetic implant is displayed on a display **19**. By way of yet another example, the vertical position of the artificial head **113** can be displayed and superimposed on a reconstructed 3D image of the natural femoral head (see **126**) of the operative hip based upon preoperative planning input images **30**, **50**, **70**. By way of still yet another example, the display **19** may optionally display a "best fit" percentage in which a percentage reaching or close to 100% reflects the alignment of an identified component of an endoprosthetic implant (*e.g.*, a femoral component **104**) relative to a reference orthopedic element.

[00143] For example, in embodiments wherein the identified component of an endoprosthetic implant is the femoral component **104**, the reference orthopedic element can be the native proximal femur **105** of the operative joint that was identified and reconstructed in accordance with any of the embodiments of this disclosure from preoperative planning input images. In such exemplary embodiments, the alignment best fit percentage can consider the anteversion angle **υ** of the identified femoral component **104**, the varus-valgus position of the femoral stem **115** of the femoral component **104** relative to the anatomical axis of the femur **105**, the anterior-posterior angle of the femoral stem **115** in the intramedullary canal of the femur **105** of the operative hip joint **101** and the vertical, horizontal, and anterior-posterior position of the artificial femoral head **113** relative to the natural femoral head (see **126**) of the operative hip joint **101** prior to resection. Combinations

of any of the forgoing embodiments of what can be displayed on the display **19** are considered to be within the scope of this disclosure.

[00144] In embodiments in which the identified component of an endoprosthetic implant is a femoral component of a hip implant and in which the identified orthopedic element is the proximal femur into which the femoral component will be inserted and seated, exemplary systems may display the varus or valgus angle of the longitudinal axis of the femoral component relative to the anatomical axis of the femur (*i.e.*, the central axis of the femur extending through the intramedullary canal of the femur).

[00145] Exemplary systems may further comprise one or more databases. One or more databases can comprise a list of types of components of an endoprosthetic implant and associated component size dimensions for the types of components (*e.g.*, different product models of a particular component) in the list of components of the endoprosthetic implant. In exemplary embodiments, a database can comprise a list of sizes for components of one particular type of component of an endoprosthetic implant.

[00146] The computational machine can compare the dimensions of the identified component of an endoprosthetic implant with the values stored in the database. The computation machine may then select or display a recommended type of component and/or a recommended size of a particular component from the values stored in the database based upon how closely the dimensions of the identified component of the endoprosthetic implant match the dimensions of the values stored in the database. In this way, a computational machine **1600** can be said to "configured to select" a recommended type of component of an endoprosthetic implant based on the determined size dimensions of the identified orthopedic element in three dimensional space. Likewise, in this way, a computational machine **1600** can be said to be "configured to recommend a size of a component of an endoprosthetic implant" based on the determined size dimensions of the identified orthopedic element in three dimensional space.

[00147] This display **19** may take the form of a screen. In other exemplary embodiments, the display **19** may comprise a glass or plastic surface that is worn or held by the surgeon or other people in the operation theater. Such a display **19** may comprise part of an augmented reality device, such that the display shows the 3D model in addition to the wearer's visual field. In certain embodiments, such a 3D model can be superimposed on the actual operative joint. In yet other exemplary embodiments, the 3D model can be "locked" to one or more features of the operative orthopedic element **100**, thereby maintaining a virtual position of the 3D model relative to the one or more features of the operative orthopedic element **100** independent of movement of the display **19**. It is still further contemplated that the display **19** may comprise part of a virtual reality system in which the entirety of the visual field is simulated.

[00148] Although X-ray radiographs from an X-ray imaging system may be desirable because X-ray radiographs are relatively inexpensive compared to CT scans and because the equipment for some X-ray imaging systems, such as a fluoroscopy system, are generally sufficiently compact to be used intraoperatively, nothing in this disclosure limits the use of the 2D images to X-ray radiographs unless otherwise expressly claimed, nor does anything in this disclosure limit the type of imaging system to an X-ray imaging system. Other 2D images can include by way of example: CT-images, CT-fluoroscopy images, fluoroscopy images, ultrasound images, positron emission tomography ("PET") images, and MRI images. Other imaging systems can include by way of example: CT, CT-fluoroscopy, fluoroscopy, ultrasound, PET, and MRI systems.

[00149] Preferably, the exemplary methods can be implemented on a computer platform (*e.g.*, a computational machine **1600**) having hardware such as one or more central processing units (CPU), a random access memory (RAM), and input/output (I/O) interface(s). An example of the architecture for an example computational machine **1600** is provided below with reference to **FIG. 7**.

[00150] **FIG. 13** generally depicts a block diagram of an exemplary computational machine **1600** upon which one or more of the methods discussed herein may be performed in accordance with some exemplary embodiments. In certain exemplary embodiments, the computational machine **1600** can operate on a single machine. In other exemplary embodiments, the computational machine **1600** can comprise connected (*e.g.*, networked) machines. Examples of networked machines that can comprise the exemplary computational machine **1600** include by way of example, cloud computing configurations, distributed hosting configurations, and other computer cluster configurations. In a networked configuration, one or more machines of the computational machine **1600** can operate in the capacity of a client machine, a server machine, or both a server-client machine. In exemplary embodiments, the computational machine **1600** can reside on a personal computer ("PC"), a mobile telephone, a tablet PC, a web appliance, a personal digital assistant ("PDA"), a network router, a bridge, a switch, or any machine capable of executing instructions that specify actions to be undertaken by said machine or a second machine controlled by said machine.

[00151] Example machines that can comprise the exemplary computational machines **1600** can include by way of example, components, modules, or like mechanisms capable of executing logic functions. Such machines may comprise tangible entities (*e.g.*, hardware) that is capable of carrying out specified operations while operating. As an example, the hardware may be hardwired (*e.g.*, specifically configured) to execute a specific operation. By way of example, such hardware may have configurable execution media (*e.g.*, circuits, transistors, logic gates, etc.) and a

computer-readable medium having instructions, wherein the instructions configure the execution media to carry out a specific operation when operating. The configuring can occur via a loading mechanism or under the direction of the execution media. The execution media selectively communicate to the computer-readable medium when the machine is operating. By way of an example, when the machine is in operation, the execution media may be configured by a first set of instructions to execute a first action or set of actions at a first point in time and then reconfigured at a second point in time by a second set of instructions to execute a second action or set of actions.

[00152] The exemplary computational machine **1600** may include a hardware processor **1697** (*e.g.*, a CPU, a graphics processing unit ("GPU"), a hardware processor core, or any combination thereof, a main memory **1696** and a static memory **1695**, some or all of which may communicate with each other via an interlink (*e.g.*, a bus) **1694**. The computational machine **1600** may further include a display unit **1698**, an input device **1691** (preferably an alphanumeric or character-numeric input device such as a keyboard), and a user interface ("UI") navigation device **1699** (*e.g.*, a mouse or stylus). In an exemplary embodiment, the input device **1691**, display unit **1698**, and UI navigation device **1699** may be a touch screen display. In exemplary embodiments, the display unit **1698** may include holographic lenses, glasses, goggles, other eyewear, or other AR or VR display components. For example, the display unit **1698** may be worn on a head of a user and may provide a heads-up-display to the user. The input device **1691** may include a virtual keyboard (*e.g.*, a keyboard displayed virtually in a virtual reality ("VR") or an augmented reality ("AR") setting) or other virtual input interface.

[00153] The computational machine **1600** may further include a storage device (*e.g.*, a drive unit) **1692**, a signal generator **1689** (*e.g.*, a speaker) a network interface device **1688**, and one or more sensors **1687**, such as a global positioning system ("GPS") sensor, accelerometer, compass, or other sensor. The computational machine **1600** may include an output controller **1684**, such as a serial (*e.g.*, universal serial bus ("USB"), parallel, or other wired or wireless (*e.g.*, infrared ("IR") near field communication ("NFC"), radio, etc.) connection to communicate or control one or more ancillary devices.

[00154] The storage device **1692** may include a machine-readable medium **1683** that is non-transitory, on which is stored one or more sets of data structures or instructions **1682** (*e.g.*, software) embodying or utilized by any one or more of the functions or methods described herein. The instructions **1682** may reside completely or at least partially, within the main memory **1696**, within static memory **1695**, or within the hardware processor **1697** during execution thereof by the computational machine **1600**. By way of example, one or any combination of the hardware processor **1697**, the main memory **1696**, the static memory **1695**, or the storage device **1692**, may constitute machine-readable media.

[00155] While the machine-readable medium **1683** is illustrated as a single medium, the term, "machine readable medium" may include a single medium or multiple media (*e.g.*, a distributed or centralized database, or associated caches and servers) configured to store the one or more instructions **1682**.

[00156] The term "machine-readable medium" may include any medium that is capable of storing, encoding, or carrying instructions for execution by the computational machine **1600** and that cause the computational machine **1600** to perform any one or more of the methods of the present disclosure, or that is capable of storing, encoding, or carrying data structures used by or associated with such instructions. A non-limited example list of machine-readable media may include magnetic media, optical media, solid state memories, non-volatile memory, such as semiconductor memory devices (*e.g.*, electronically erasable programmable read-only memory ("EEPROM"), electronically programmable read-only memory ("EPROM"), and magnetic discs, such as internal hard discs and removable discs, flash storage devices, magneto-optical discs, and CD-ROM and DVD-ROM discs.

[00157] The instructions **1682** may further be transmitted or received over a communications network **1681** using a transmission medium via the network interface device **1688** utilizing any one of a number of transfer protocols (*e.g.*, internet protocol ("IP"), user datagram protocol ("UDP"), frame relay, transmission control protocol ("TCP"), hypertext transfer protocol ("HTTP"), etc.). Example communication networks may include a wide area network ("WAN"), a plain old telephone ("POTS") network, a local area network ("LAN"), a packet data network, a mobile telephone network, a wireless data network, and a peer-to-peer ("P2P") network. By way of example, the network interface device **1688** may include one or more physical jacks (*e.g.*, Ethernet, coaxial, or phone jacks) or one or more antennas to connect to the communications network **1681**.

[00158] By way of example, the network interface device **1688** may include a plurality of antennas to communicate wirelessly using at least one of a single-input multiple-output ("SIMO"), or a multiple-input single output ("MISO") methods. The phrase, "transmission medium" includes any intangible medium that is capable of storing, encoding, or carrying instructions for execution by the computational machine **1600**, and includes analog or digital communications signals or other intangible medium to facilitate communication of such software.

[00159] Exemplary methods in accordance with this disclosure may be machine or computer-implemented at least in part. Some examples may include a computer-readable medium or machine-readable medium encoded with instructions operable to configure an electronic device to perform the exemplary methods described herein. An example implementation of such an exemplary method may include code, such as assembly language code, microcode, a higher-level

language code, or other code. Such code may include computer readable instructions for performing various methods. The code may form portions of computer program products. A computational machine **1600** that can execute computer readable instructions for carrying out the methods and calculations of a deep learning network can be said to be "configured to run" a deep learning network. Further, in an example, the code may be tangibly stored on or in a volatile, non-transitory, or non-volatile tangible computer-readable media, such as during execution or other times. Examples of these tangible computer-readable media may include, but are not limited to, removable optical discs (*e.g.*, compact discs and digital video discs), hard drives, removable magnetic discs, memory cards or sticks, include removable flash storage drives, magnetic cassettes, random access memories (RAMs), read only memories (ROMS), and other media.

[00160] It is further contemplated that the exemplary methods disclosed herein may be used for preoperative planning, intraoperative planning or execution, or postoperative evaluation of the implant placement and function.

[00161] An exemplary method for ascertaining a position of an orthopedic element in space can comprise: calibrating a radiographic imaging machine to determine a mapping relationship between image points and corresponding space coordinates to define spatial data; capturing a first image of an orthopedic element using a radiographic imaging technique, wherein the first image defines a first reference frame; capturing a second image of the orthopedic element using the radiographic imaging technique, wherein the second image defines a second reference frame, and wherein the first reference frame is offset from the second reference frame at an offset angle; using a deep learning network to detect the orthopedic element using the spatial data, the spatial data defining anatomical landmarks on or in the orthopedic element; using the deep learning network to apply a mask to the orthopedic element defined by an anatomical landmark; projecting the spatial data from the first image of the desired orthopedic element and the spatial data from the second image of the desired orthopedic element to define volume data, wherein the spatial data comprising image points disposed within a masked area of either the first image or the second image have a first value and wherein the spatial data comprising image points disposed outside of the masked area of either the first image or the second image have a second value, wherein the first value is different from the second value; applying the deep learning network to the volume data to generate a reconstructed three-dimensional model of the orthopedic element; and mapping the three-dimensional model of the orthopedic element to the spatial data.

[00162] In an exemplary embodiment, an exemplary method can further comprise using the deep learning network to perform a style transfer on the first image and the second image. In an exemplary embodiment, the style transfer converts the spatial data from the radiographic imaging technique into dynamic digital radiography data.

[00163] In an exemplary embodiment, the first value is a positive value.

[00164] In an exemplary embodiment, the second value is a negative value.

[00165] In an exemplary embodiment, the exemplary method further comprises projecting the reconstructed three-dimensional model on a display.

[00166] In an exemplary embodiment, the deep learning network comprises a convolutional neural network.

[00167] In an exemplary embodiment, the radiographic imaging technique is fluoroscopy.

[00168] In an exemplary embodiment, the method is performed intraoperatively.

[00169] In an exemplary embodiment, the orthopedic element is an acetabulum of a pelvis.

[00170] In an exemplary embodiment, the exemplary method further comprises calculating a center of the acetabulum.

[00171] In an exemplary embodiment, the exemplary method further comprises aligning a longitudinal rotational axis of a neck of the femoral stem (*e.g.*, a component of an endoprosthetic implant) with the center of the acetabulum.

[00172] In an exemplary embodiment, the exemplary method further comprises aligning the acetabular shell (*e.g.*, a component of an endoprosthetic implant) with the reamed acetabulum of the patient.

[00173] In an exemplary embodiment, the exemplary method further comprises aligning the femoral stem (*e.g.*, a component of an endoprosthetic implant) in the intramedullary canal of the reamed proximal femur of the patient.

[00174] In an exemplary embodiment, the method further comprises aligning a longitudinal axis of a femoral stem (*e.g.*, a component of an endoprosthetic implant) with the anatomical (*i.e.*, center) axis of the femur.

[00175] An exemplary method for ascertaining a position of an orthopedic element in space comprises: calibrating a radiographic imaging machine to determine a mapping relationship between image points and corresponding space coordinates to define spatial data; using a radiographic imaging technique to capture a first image of an orthopedic element, wherein the first image defines a first reference frame; using the radiographic imaging technique to capture a second image of the orthopedic element, wherein the second image defines a second reference frame, and wherein the first reference frame is offset from the second reference frame at an offset angle; using a neural network to detect the orthopedic element using the spatial data, the spatial data defining an anatomical landmark on or in the orthopedic element; using the deep learning network to apply a mask to the orthopedic element defined by the anatomical landmark; projecting the spatial data

from the first image of the desired orthopedic element and the spatial data from the second image of the desired orthopedic element to define volume data, wherein the spatial data comprising image points disposed within a masked area of either the first image or the second image have a positive value and wherein the spatial data comprising image points disposed outside of a masked area of either the first image or the second image have a negative value; applying the deep learning network to the volume data to generate a three-dimensional model of the orthopedic element; and mapping the three-dimensional model of the orthopedic element to the spatial data, wherein the orthopedic element is an acetabulum of a pelvis.

[00176] In an exemplary embodiment, the orthopedic element is resected or reamed during a surgical procedure.

[00177] In an exemplary embodiment, the method further comprises using the deep learning network to perform a style transfer on the first image and the second image.

[00178] In an exemplary embodiment, the style transfer converts the spatial data from the radiographic imaging technique into dynamic digital radiography data.

[00179] In an exemplary embodiment, the first value is a positive value.

[00180] In an exemplary embodiment, the second value is a negative value.

[00181] In an exemplary embodiment, the method further comprises projecting the reconstructed three-dimensional model on a display.

[00182] In an exemplary embodiment, the deep learning network comprises a convolutional neural network.

[00183] In an exemplary embodiment, the radiographic imaging technique is fluoroscopy.

[00184] In an exemplary embodiment, the method is performed intraoperatively.

[00185] In an exemplary embodiment, the method further comprises calculating a center of the acetabulum.

[00186] In an exemplary embodiment, the method further comprises aligning a longitudinal rotational axis of a neck of femoral stem rotationally with a center of the artificial femoral head and the longitudinal axis of the femoral stem with the anatomical axis of the intramedullary canal of the femur into which the femoral stem is placed.

[00187] In an exemplary embodiment, the exemplary method further comprises aligning the acetabular shell (*e.g.,* a component of an endoprosthetic implant) with the reamed acetabulum of the patient.

[00188] In an exemplary embodiment, the exemplary method further comprises aligning the femoral stem (*e.g.,* a component of an endoprosthetic implant) in the intramedullary canal of the reamed proximal femur of the patient.

[00189] In an exemplary embodiment, the method further comprises aligning a longitudinal axis of a femoral stem (*e.g.*, a component of an endoprosthetic implant) with the anatomical axis of the femur into which the femoral stem is placed.

[00190] An exemplary system for ascertaining a position of an orthopedic element and a component of an endoprosthetic implant in space comprises: a tissue-penetrating imaging machine; a first input image, the first input image taken by the tissue penetrating imaging machine from a first reference frame, the first image depicting a calibration jig; a second input image, the second input image taken by the tissue penetrating imaging machine from a second reference frame, the second reference frame being offset from the first reference frame, the second image depicting the calibration jig; and a computational machine configured to run a deep learning network, wherein the deep learning network is configured to identify an orthopedic element and a component of an endoprosthetic implant to define an identified orthopedic element and an identified component of the endoprosthetic implant, and to map the identified orthopedic element and the identified component of the endoprosthetic implant to spatial data ascertained by the first input image and the second input image to thereby determine the position of the identified orthopedic element and the identified component of the endoprosthetic implant in three dimensional space.

[00191] In an exemplary embodiment, the system further comprises a third input image, the third input image is taken by the tissue penetrating imaging machine from a third reference frame, the third image depicting the calibration jig.

[00192] In an exemplary embodiment of the system, the deep learning network is further configured to identify multiple orthopedic elements and multiple components of the endoprosthetic implant to define multiple identified orthopedic elements and multiple identified components of the endoprosthetic implant.

[00193] In still further exemplary embodiments of the system, a first identified component of the multiple identified components of the endoprosthetic implant is an acetabular component of a hip endoprosthetic implant and a second identified component of the multiple identified components of the endoprosthetic implant is a femoral component of a hip endoprosthetic implant.

[00194] In an exemplary embodiment of the system, the identified component of the endoprosthetic implant is an acetabular shell and the identified orthopedic element is a reamed acetabulum proximate to the acetabular shell.

[00195] In an exemplary embodiment of the system, the identified component of the endoprosthetic implant is a femoral stem and the identified orthopedic element is an intramedullary canal of a femur proximate to the femoral stem.

[00196] In an exemplary embodiment of the system, the identified orthopedic element is modeled in three dimensions to define a modeled orthopedic element.

[00197] In an exemplary embodiment, the modeled orthopedic element is displayed on a display.

[00198] In an exemplary embodiment, the identified component of the endoprosthetic implant is modeled in three dimensions to define a modeled component of the endoprosthetic implant.

[00199] In an exemplary embodiment, the modeled component of the endoprosthetic implant is displayed on a display.

[00200] In an exemplary embodiment, a calculated abduction angle of the identified component of the endoprosthetic implant is displayed on a display.

[00201] In an exemplary embodiment, a calculated anteversion angle of the identified component of the endoprosthetic implant is displayed on a display.

[00202] An exemplary system for recommending a type of a component of an endoprosthetic implant to be surgically implanted into a patient, the system comprising: a tissue penetrating imaging machine; a first input image, the first input image taken by the tissue penetrating imaging machine from a first reference frame, the first image depicting a calibration jig; a second input image, the second input image taken by the tissue penetrating imaging machine from a second reference frame, the second reference frame being offset from the first reference frame, the second image depicting the calibration jig; a computational machine configured to run a deep learning network, wherein the deep learning network is configured to identify an orthopedic element to define an identified orthopedic element, and to map the identified orthopedic element to spatial data ascertained by the first input image and the second input image to thereby define determined size dimensions of the identified orthopedic element in three dimensional space; and a database, the database comprising a list of types of components of an endoprosthetic implant and associated component size dimensions for the types of components in the list of components of the endoprosthetic implant, wherein the computational machine is further configured to select a recommended type of component of an endoprosthetic implant based on the determined size dimensions of the identified orthopedic element in three dimensional space.

[00203] In an exemplary embodiment, the system further comprises a third input image, the third input image is taken by the tissue penetrating imaging machine from a third reference frame, the third image depicting the calibration jig.

[00204] In an exemplary embodiment, the identified orthopedic element is the internal geometry of a bone before or after reaming or before or after broaching.

[00205] In an exemplary embodiment, the computational machine is configured to run a best fit algorithm to select a recommended component of an endoprosthetic implant based on the determined size dimensions of the identified orthopedic element.

[00206] An exemplary system for determining the size of a component of an endoprosthetic implant to be surgically implanted into a patient, the system comprising: a tissue penetrating imaging machine; a first input image, the first input image taken by the tissue penetrating imaging machine from a first reference frame, the first image depicting a calibration jig; a second input image, the second input image taken by the tissue penetrating imaging machine from a second reference frame, the second reference frame being offset from the first reference frame, the second image depicting the calibration jig; a computational machine configured to run a deep learning network, wherein the deep learning network is configured to identify an orthopedic element to define an identified orthopedic element, and to map the identified orthopedic element to spatial data ascertained by the first input image and the second input image to thereby define determined size dimensions of the identified orthopedic element in three dimensional space; and a database, the database comprising a list of components of an endoprosthetic implant and associated component size dimensions for the components in the list of components of the endoprosthetic implant, wherein the computational machine is further configured to recommend a size of a component of an endoprosthetic implant based on the determined size dimensions of the identified orthopedic element in three dimensional space.

[00207] In an exemplary embodiment, the system further comprises a third input image, the third input image being taken by the tissue penetrating imaging machine from a third reference frame, the third image depicting the calibration jig.

[00208] In an exemplary embodiment, the identified orthopedic element is the internal geometry of a bone before or after reaming or before or after broaching.

[00209] In an exemplary embodiment, the computational machine is configured to run a best fit algorithm to select a recommended component of an endoprosthetic implant based on the determined size dimensions of the identified orthopedic element.

[00210] It is to be understood that the present invention is by no means limited to the particular constructions and method steps herein disclosed or shown in the drawings, but also comprises any modifications or equivalents within the scope of the claims known in the art. It will be appreciated by those skilled in the art that the devices and methods herein disclosed will find utility.

CLAIMS

What is claimed is:

1. A system for ascertaining a position of an orthopedic element and a component of an endoprosthetic implant in space comprising:

a tissue-penetrating imaging machine;

a first input image, the first input image taken by the tissue penetrating imaging machine from a first reference frame, the first image depicting a calibration jig;

a second input image, the second input image taken by the tissue penetrating imaging machine from a second reference frame, the second reference frame being offset from the first reference frame, the second image depicting the calibration jig; and

a computational machine configured to run a deep learning network, wherein the deep learning network is configured to identify an orthopedic element and a component of an endoprosthetic implant to define an identified orthopedic element and an identified component of the endoprosthetic implant, and to map the identified orthopedic element and the identified component of the endoprosthetic implant to spatial data ascertained by the first input image and the second input image to thereby determine the position of the identified orthopedic element and the identified component of the endoprosthetic implant in three dimensional space.

2. The system of claim 1 further comprising a third input image, the third input image taken by the tissue penetrating imaging machine from a third reference frame, the third image depicting the calibration jig.

3. The system according to any of claims 1 to 2, wherein the deep learning network is further configured to identify multiple orthopedic elements and multiple components of the endoprosthetic implant to define multiple identified orthopedic elements and multiple identified components of the endoprosthetic implant.

4. The system of claim 3, wherein a first identified component of the multiple identified components of the endoprosthetic implant is an acetabular component of a hip endoprosthetic implant and wherein a second identified component of the multiple identified components of the endoprosthetic implant is a femoral component of a hip endoprosthetic implant.

5. The system according to any of claims 1 to 4, wherein the identified component of the endoprosthetic implant is an acetabular shell and wherein the identified orthopedic element is a reamed acetabulum proximate to the acetabular shell.

6. The system according to any of claims 1 to 5, wherein the identified component of the endoprosthetic implant is a femoral stem and wherein the identified orthopedic element is an intramedullary canal of a femur proximate to the femoral stem.

7. The system according to any of claims 1 to 6, wherein the identified orthopedic element is modeled in three dimensions to define a modeled orthopedic element.

8. The system of claim 7, wherein the modeled orthopedic element is displayed on a display.

9. The system according to any of claims 1 to 8, wherein the identified component of the endoprosthetic implant is modeled in three dimensions to define a modeled component of the endoprosthetic implant.

10. The system of claim 9, wherein the modeled component of the endoprosthetic implant is displayed on a display.

11. The system according to any of claims 1 to 10, wherein a calculated abduction angle of the identified component of the endoprosthetic implant is displayed on a display.

12. The system according to any of claims 1 to 11, wherein a calculated anteversion angle of the identified component of the endoprosthetic implant is displayed on a display.

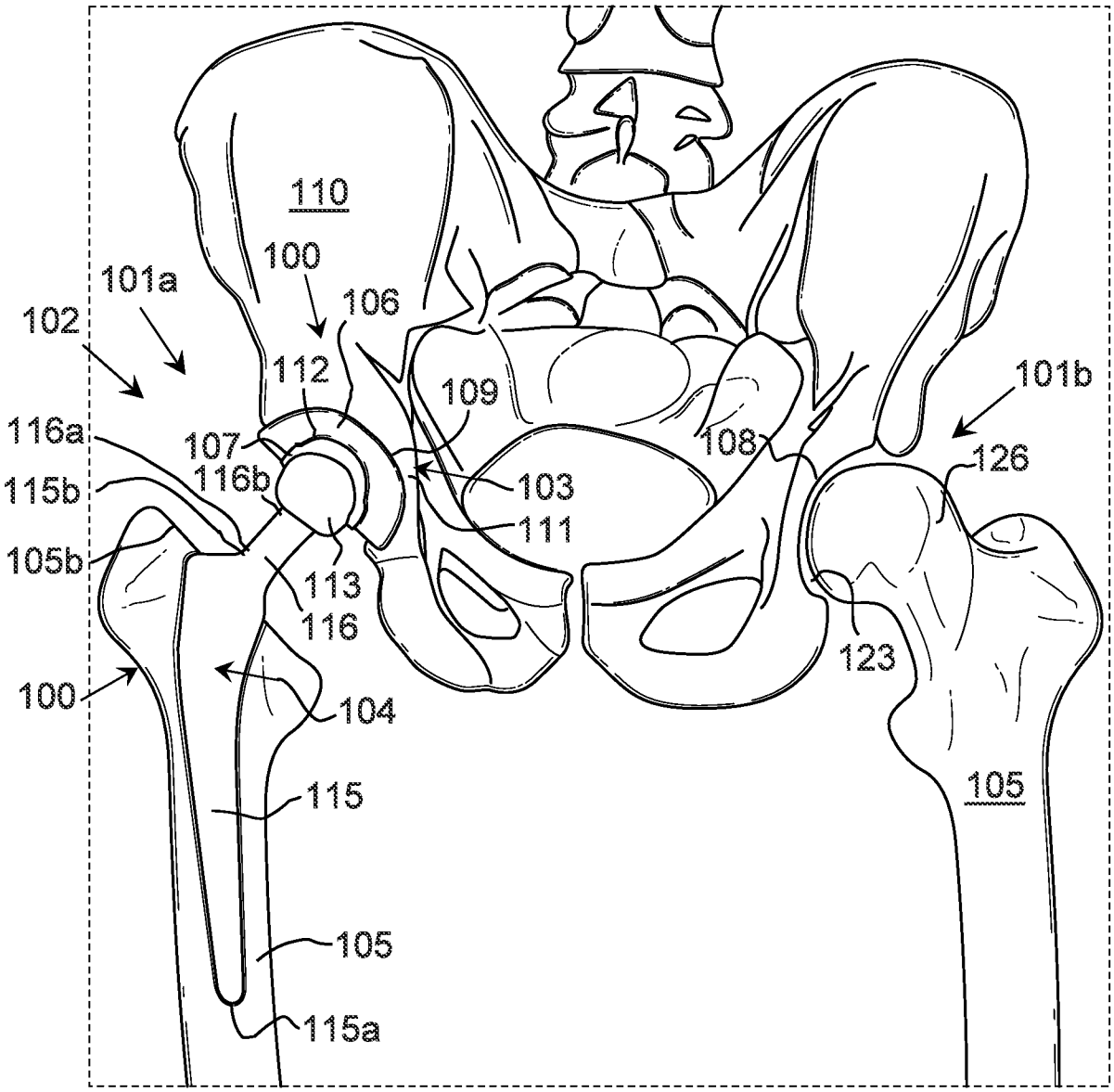
110
100
101a
102
106
112
109
101b
116a
107
108
126
115b
116b
103
111
105b
113
116
123
100
104
115
105
105
115a

FIG. 1

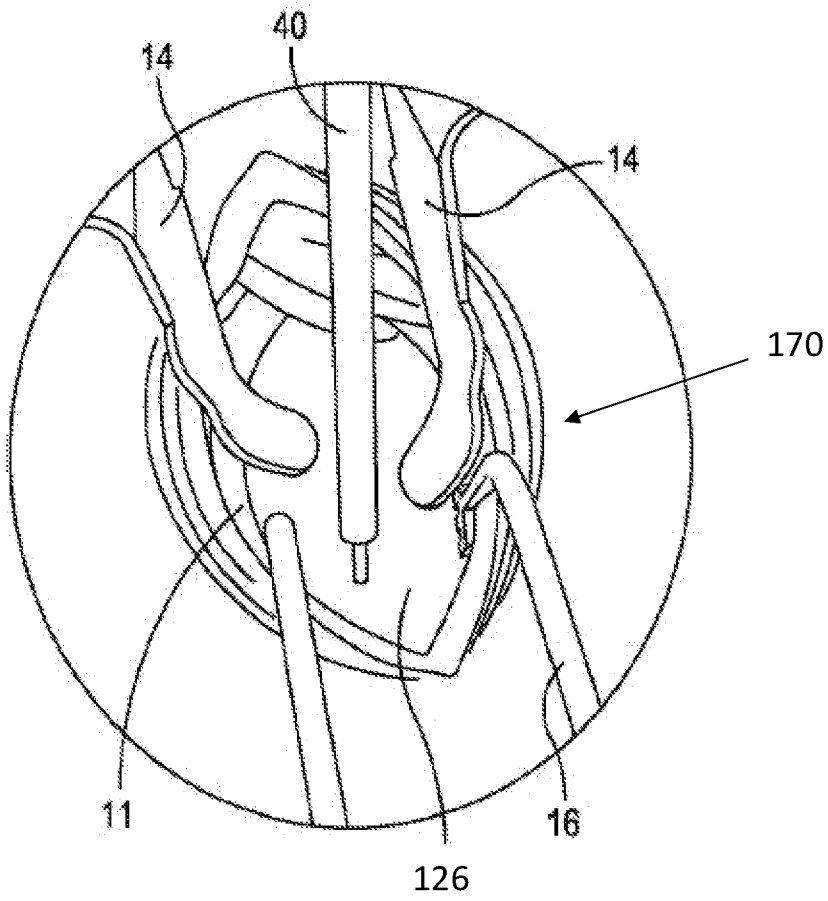

FIG. 2

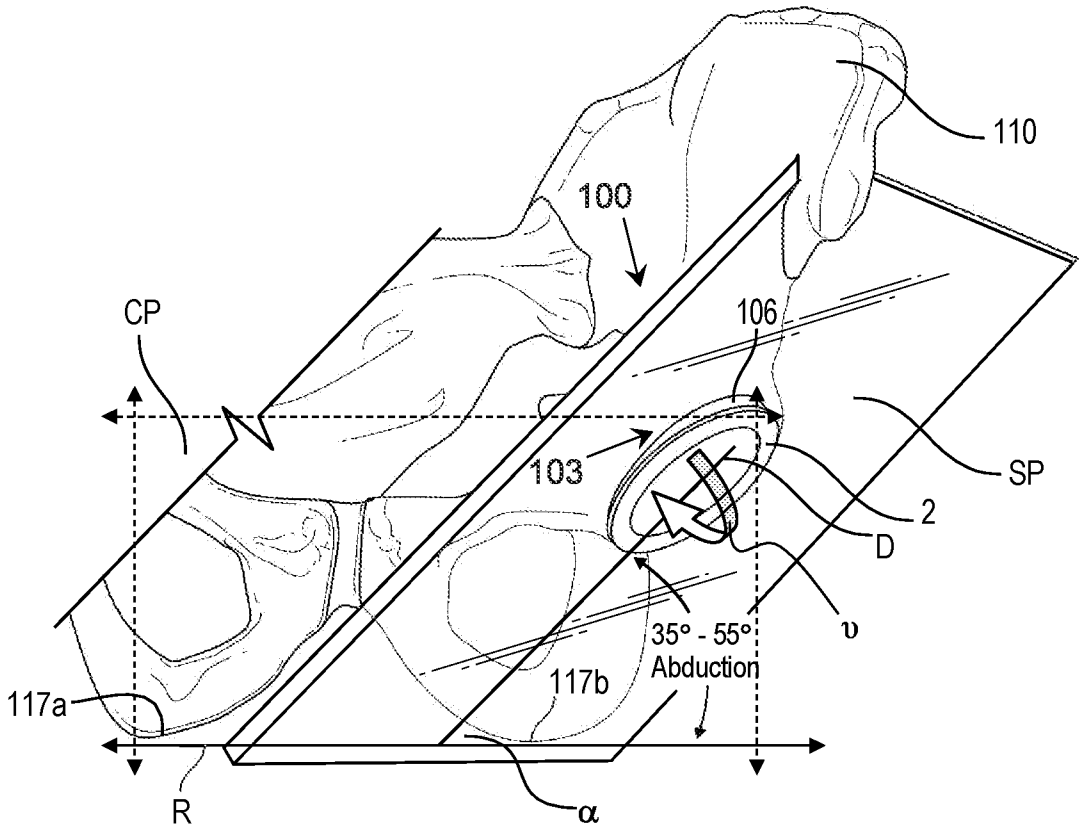

FIG. 3

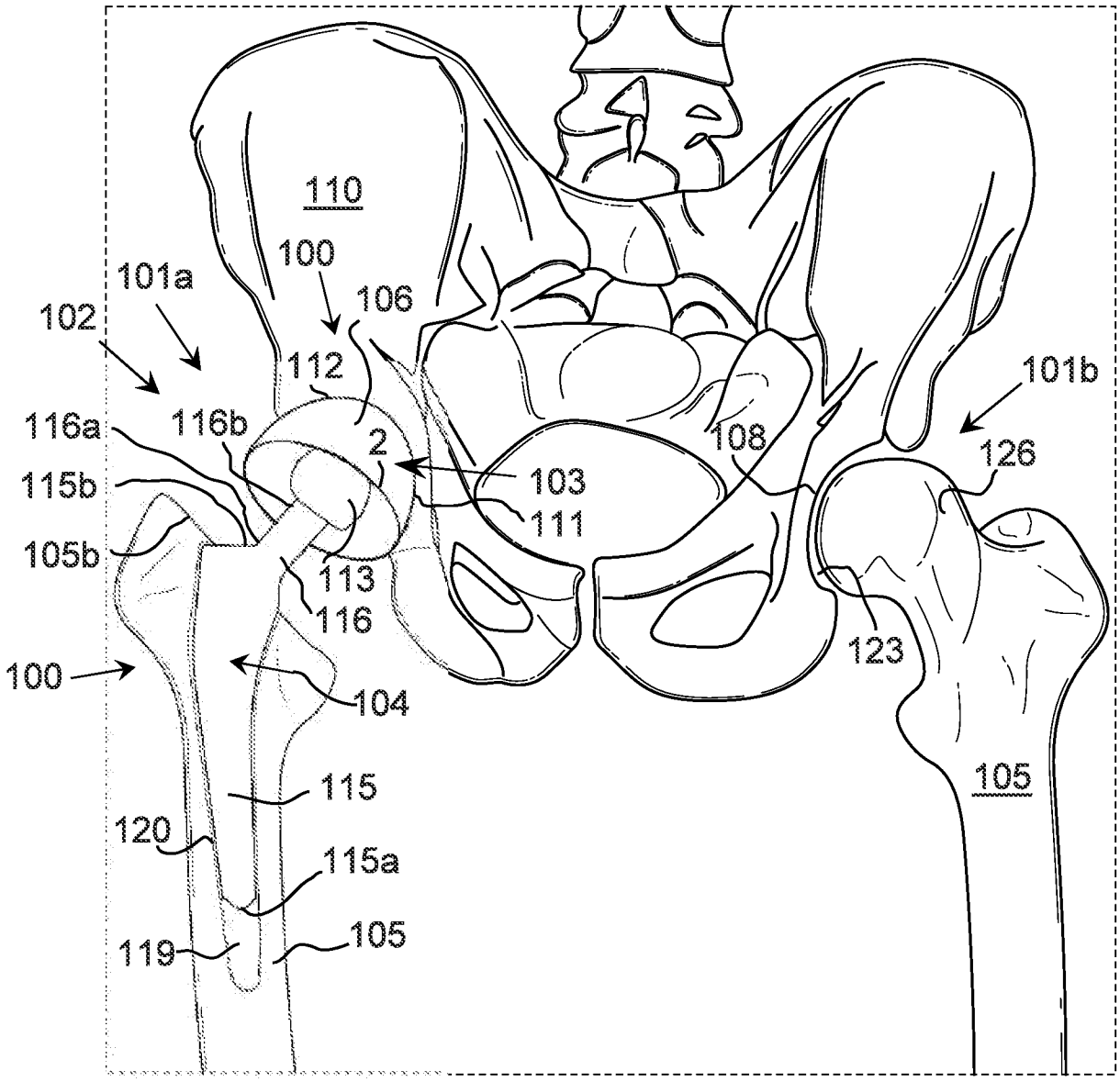
110
100
101a
102
106
112
116a
116b
2
115b
103
111
105b
113
116
100
104
115
120
115a
119
105
108
101b
126
123
105

FIG. 4

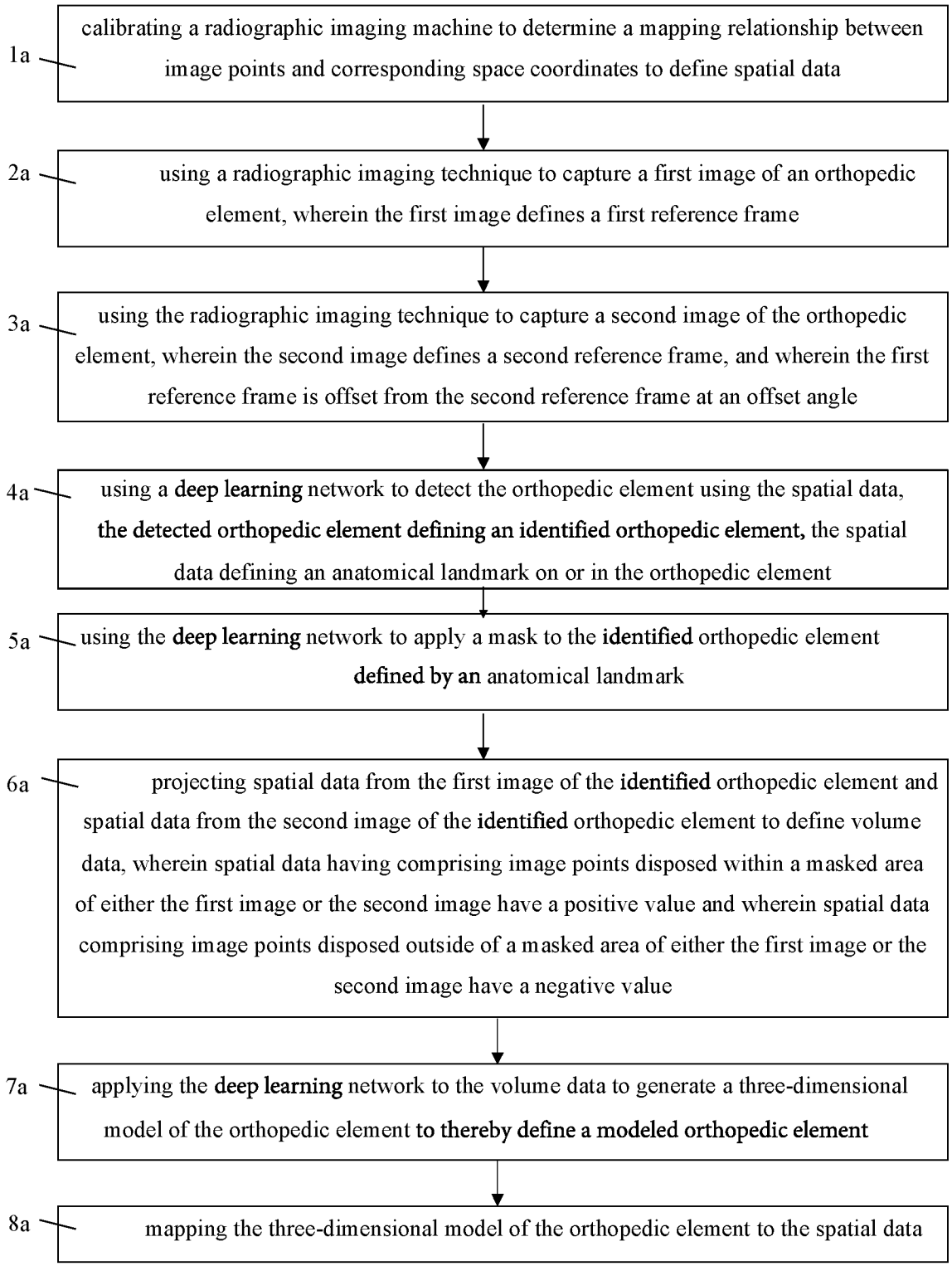
1a
calibrating a radiographic imaging machine to determine a mapping relationship between image points and corresponding space coordinates to define spatial data
2a
using a radiographic imaging technique to capture a first image of an orthopedic element, wherein the first image defines a first reference frame
3a
using the radiographic imaging technique to capture a second image of the orthopedic element, wherein the second image defines a second reference frame, and wherein the first reference frame is offset from the second reference frame at an offset angle
4a
using a deep learning network to detect the orthopedic element using the spatial data, the detected orthopedic element defining an identified orthopedic element, the spatial data defining an anatomical landmark on or in the orthopedic element
5a
using the deep learning network to apply a mask to the identified orthopedic element defined by an anatomical landmark
6a
projecting spatial data from the first image of the identified orthopedic element and spatial data from the second image of the identified orthopedic element to define volume data, wherein spatial data having comprising image points disposed within a masked area of either the first image or the second image have a positive value and wherein spatial data comprising image points disposed outside of a masked area of either the first image or the second image have a negative value
7a
applying the deep learning network to the volume data to generate a three-dimensional model of the orthopedic element to thereby define a modeled orthopedic element
8a
mapping the three-dimensional model of the orthopedic element to the spatial data

FIG. 5

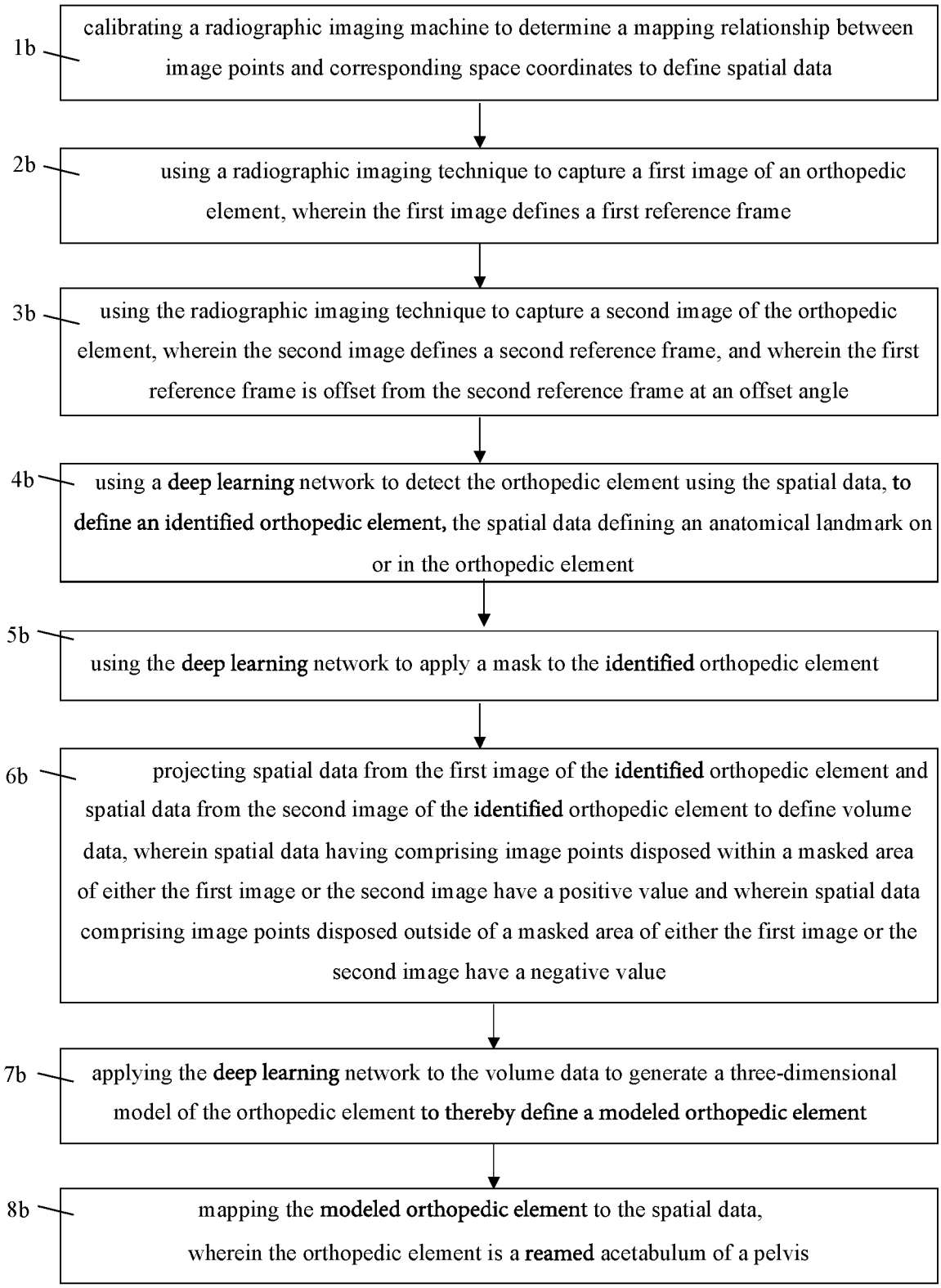
1b
calibrating a radiographic imaging machine to determine a mapping relationship between image points and corresponding space coordinates to define spatial data
2b
using a radiographic imaging technique to capture a first image of an orthopedic element, wherein the first image defines a first reference frame
3b
using the radiographic imaging technique to capture a second image of the orthopedic element, wherein the second image defines a second reference frame, and wherein the first reference frame is offset from the second reference frame at an offset angle
4b
using a deep learning network to detect the orthopedic element using the spatial data, to define an identified orthopedic element, the spatial data defining an anatomical landmark on or in the orthopedic element
5b
using the deep learning network to apply a mask to the identified orthopedic element
6b
projecting spatial data from the first image of the identified orthopedic element and spatial data from the second image of the identified orthopedic element to define volume data, wherein spatial data having comprising image points disposed within a masked area of either the first image or the second image have a positive value and wherein spatial data comprising image points disposed outside of a masked area of either the first image or the second image have a negative value
7b
applying the deep learning network to the volume data to generate a three-dimensional model of the orthopedic element to thereby define a modeled orthopedic element
8b
mapping the modeled orthopedic element to the spatial data, wherein the orthopedic element is a reamed acetabulum of a pelvis

FIG. 6

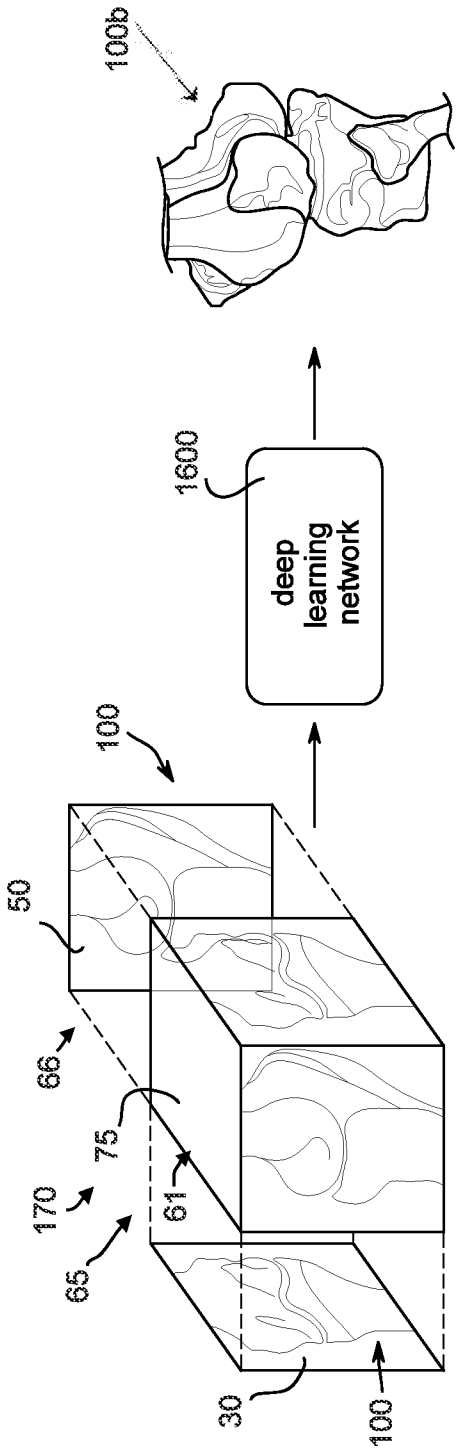

FIG.7

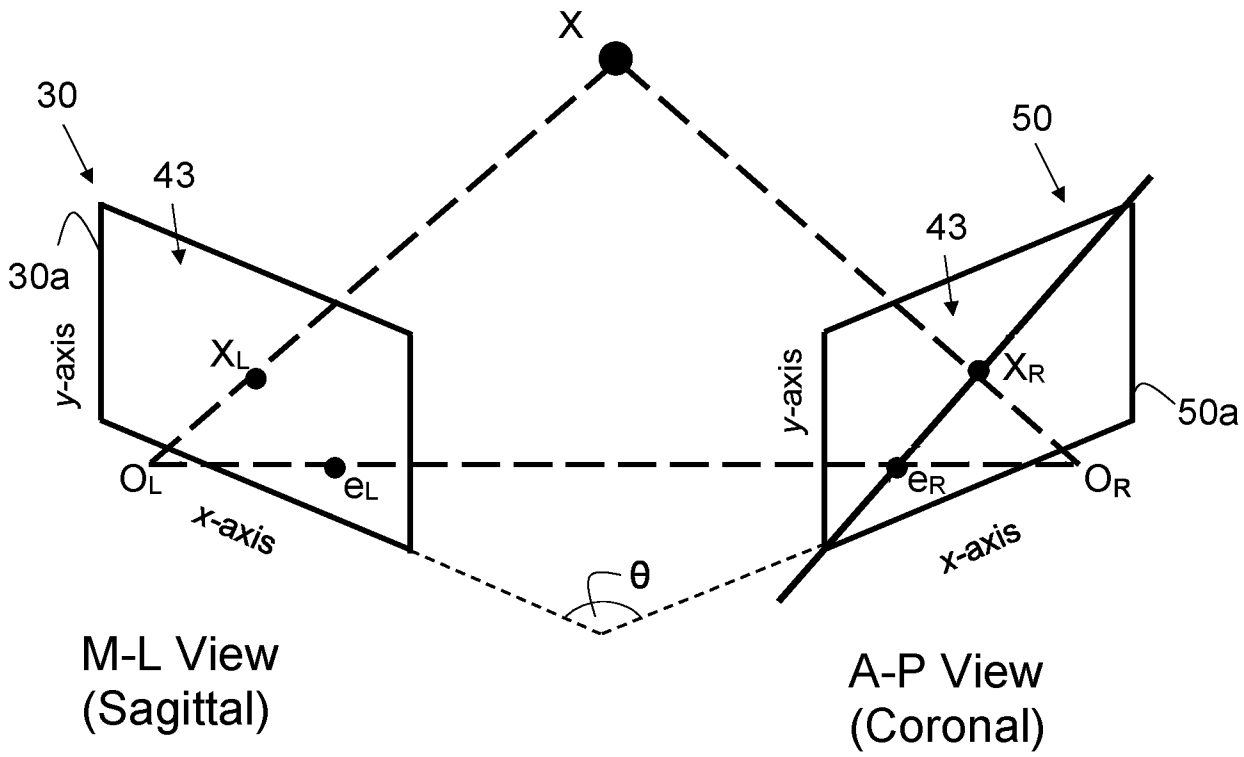
X
30
43
30a
y-axis
X_L
O_L
e_L
x-axis
θ
50
43
y-axis
X_R
50a
e_R
O_R
x-axis
M-L View
(Sagittal)
A-P View
(Coronal)

FIG. 8

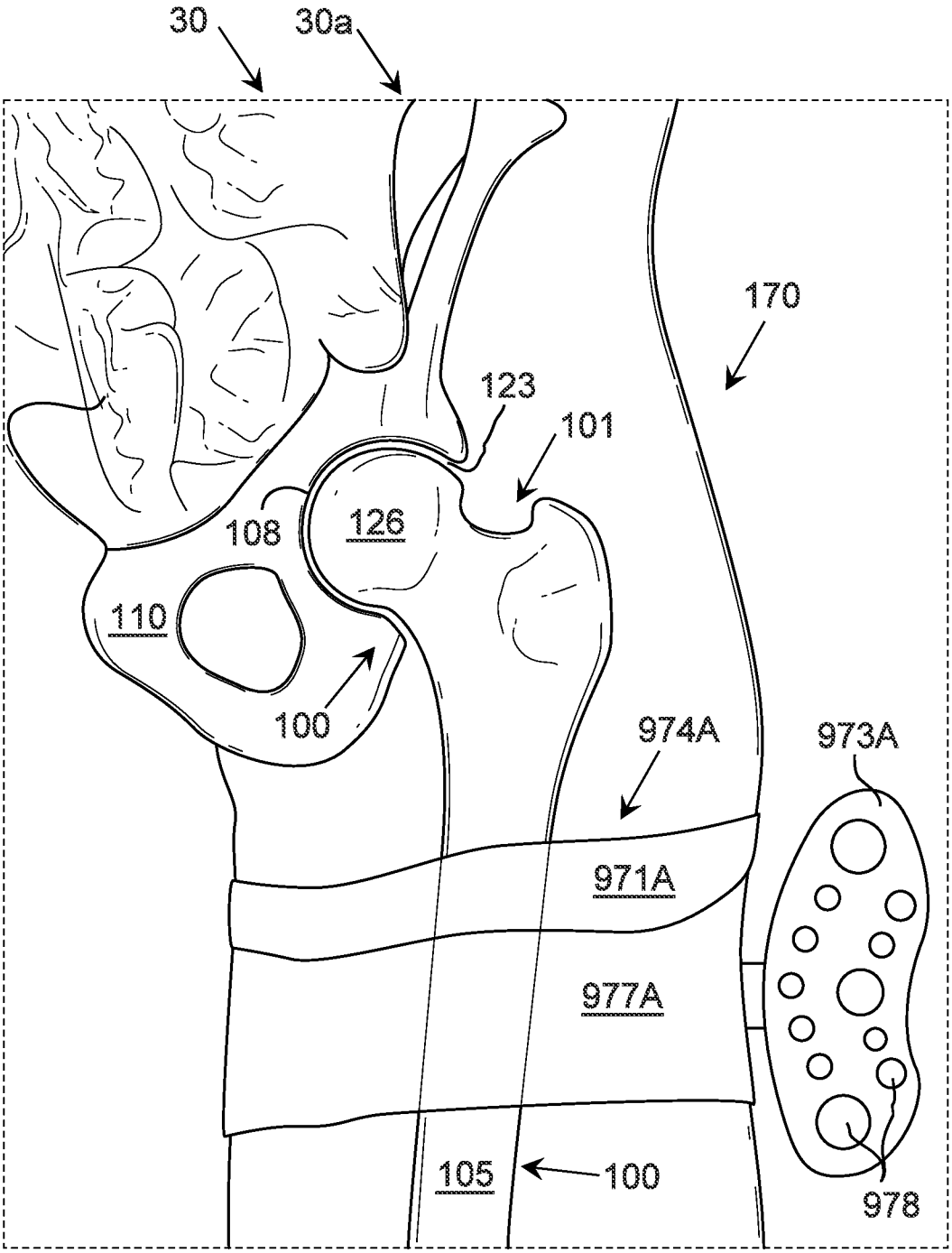
30
30a
170
123
101
108
126
110
100
974A
973A
971A
977A
105
100
978

FIG. 9A

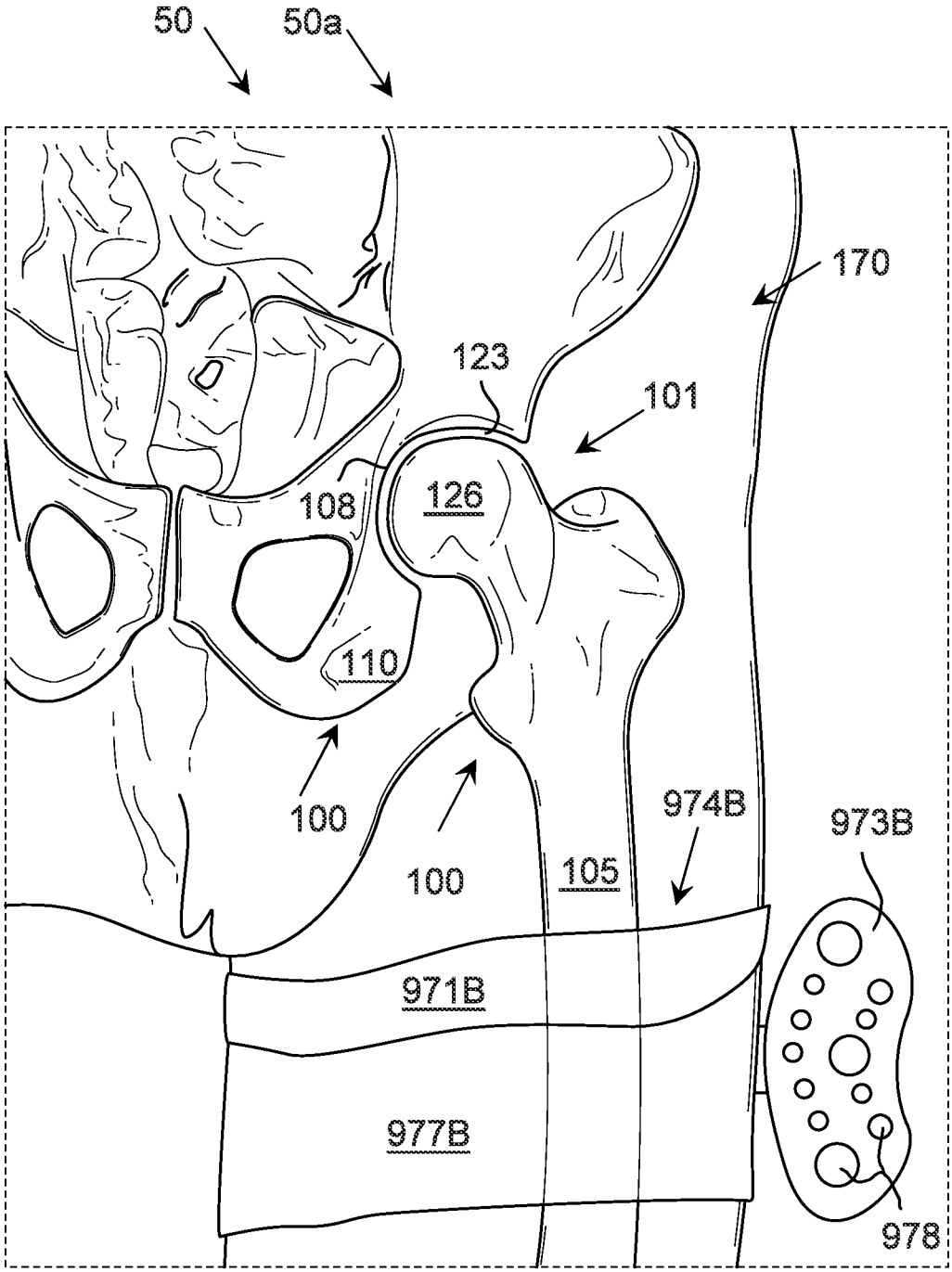
50
50a
170
123
101
108
126
110
100
100
105
974B
973B
971B
977B
978

FIG. 9B

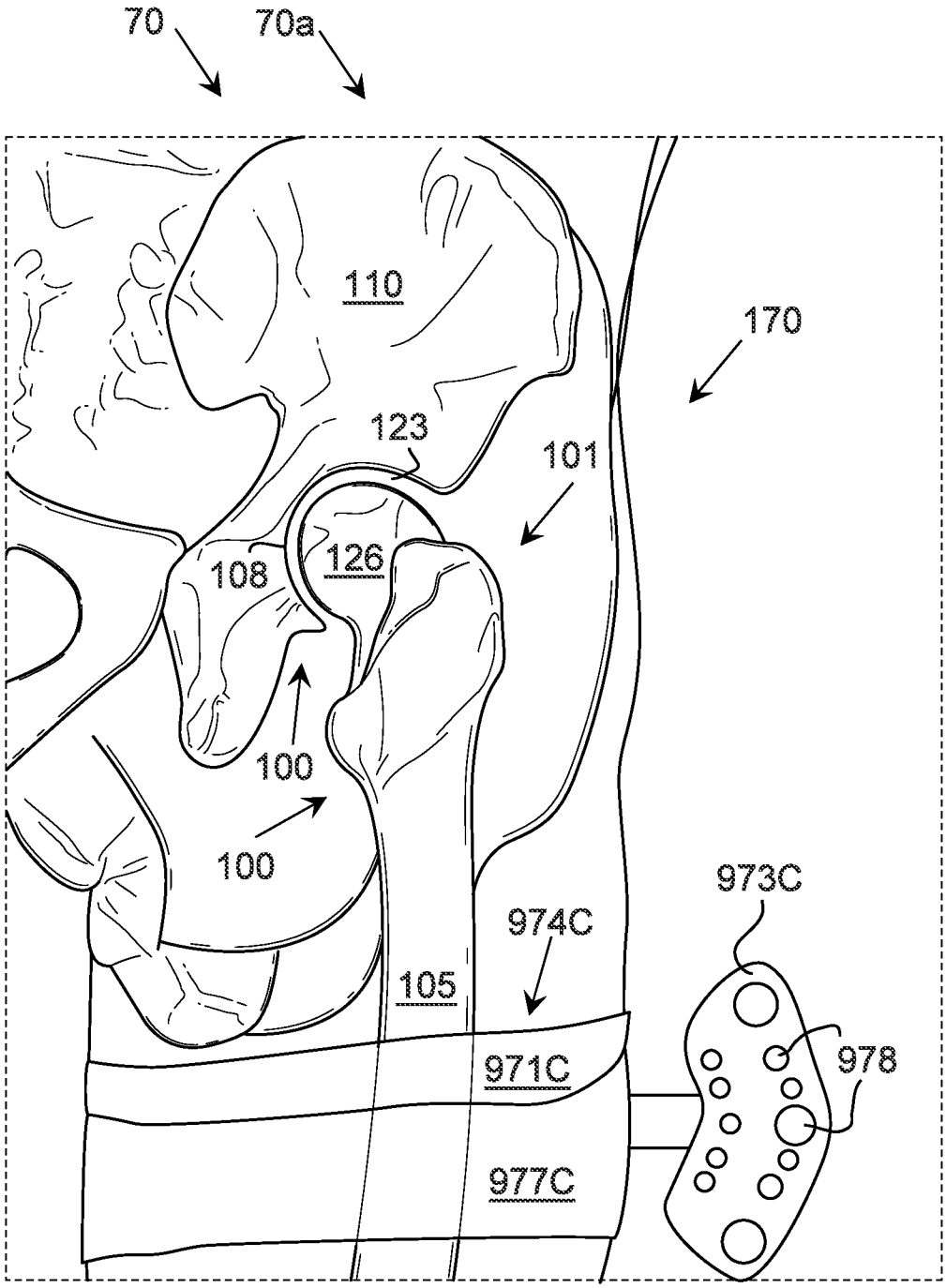
70
70a
110
170
123
101
108
126
100
100
973C
974C
105
978
971C
977C

FIG. 9C

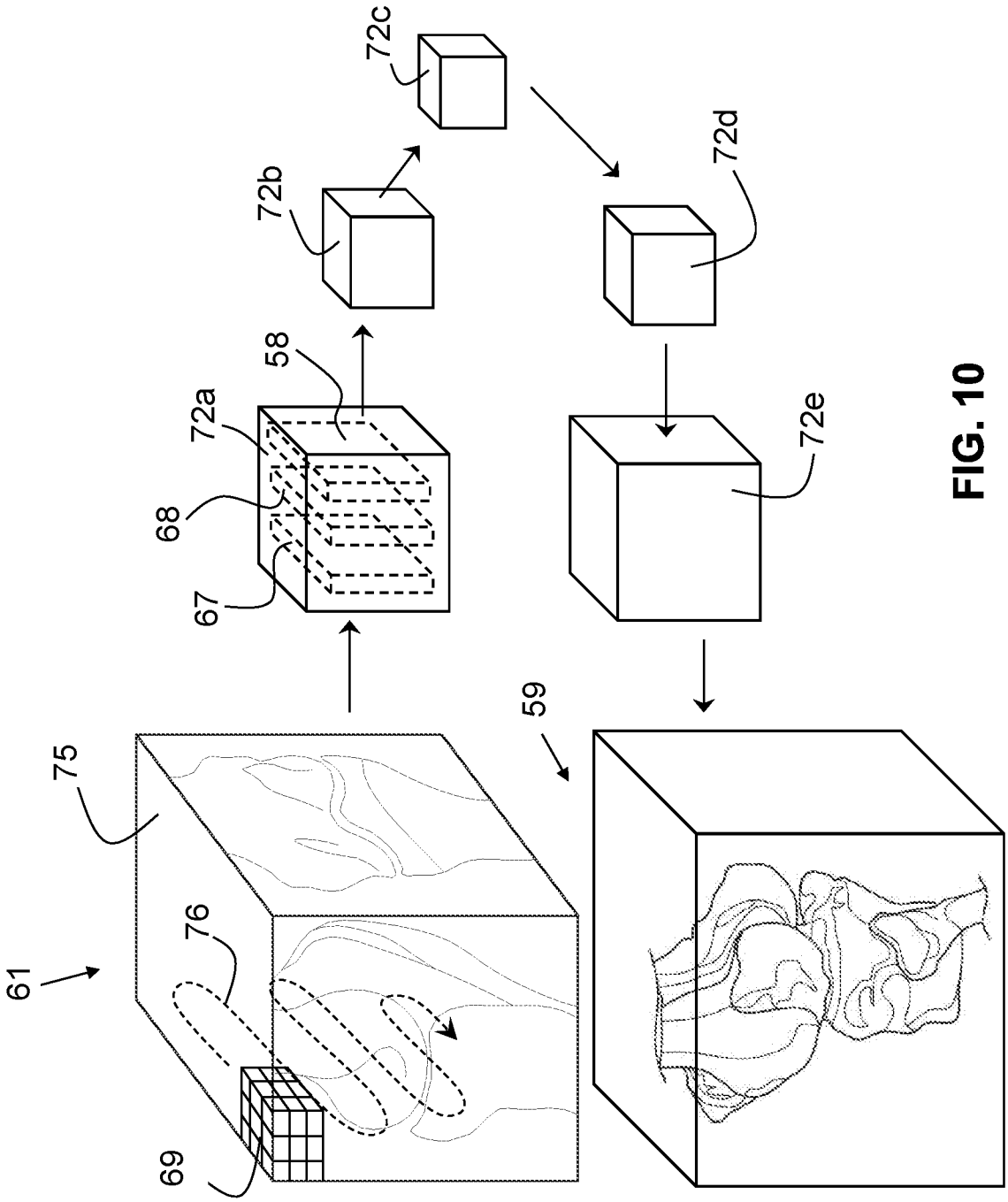

FIG. 10

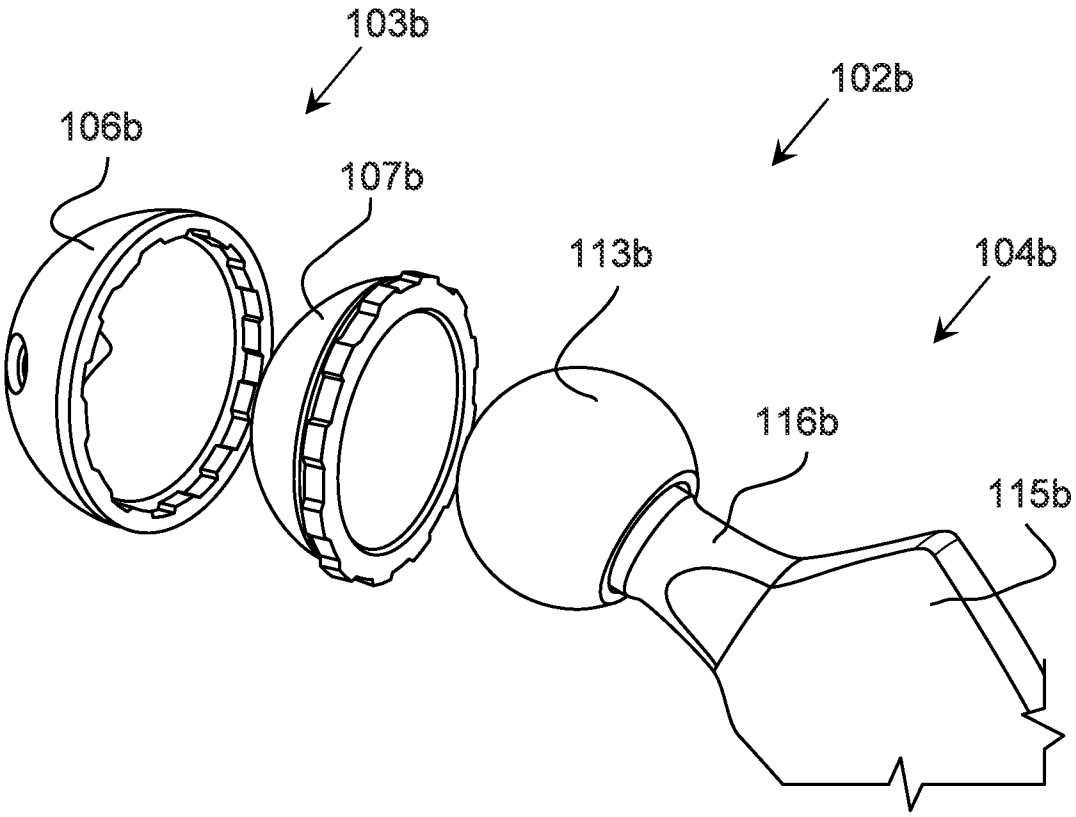

FIG. 11

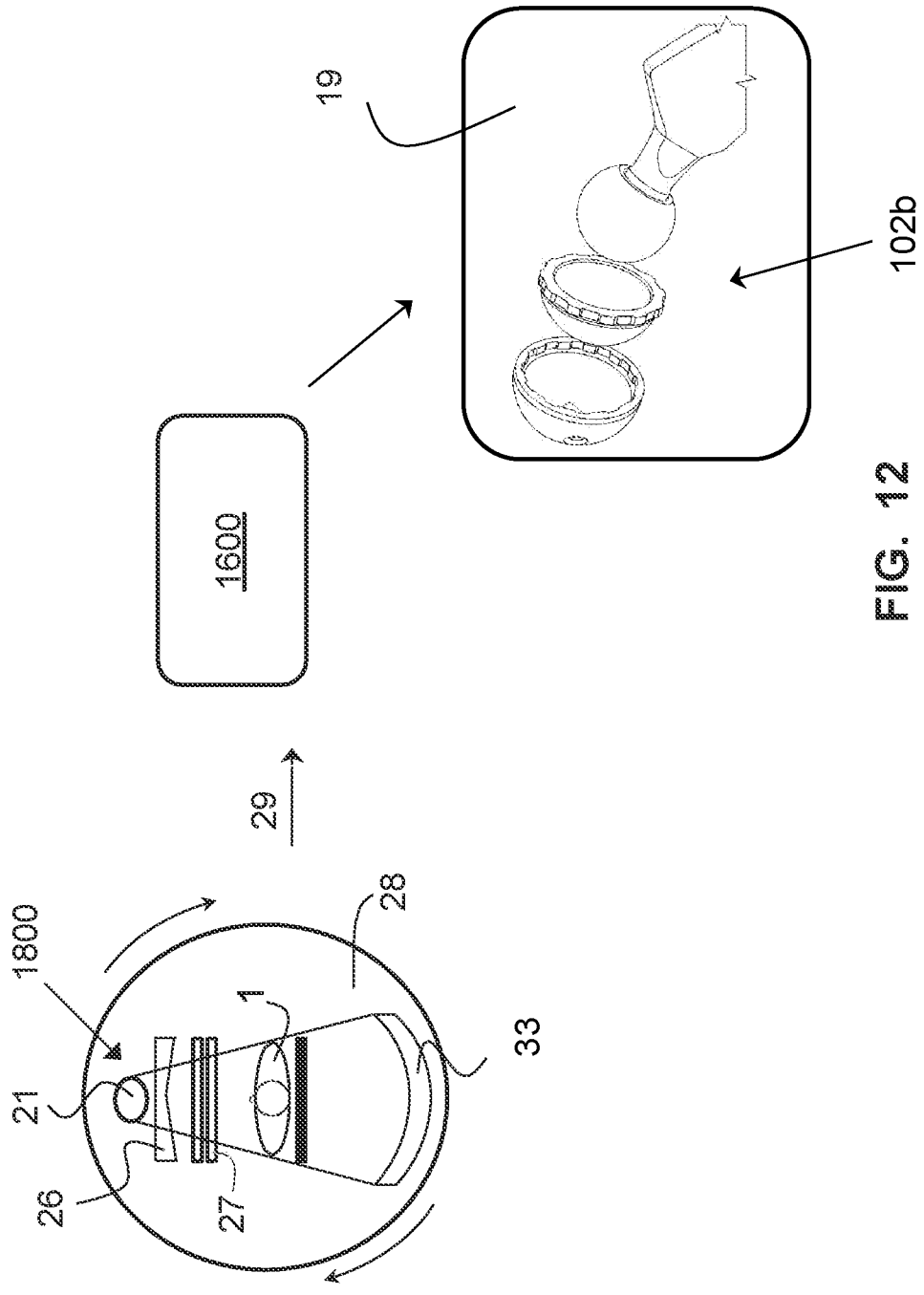

FIG. 12

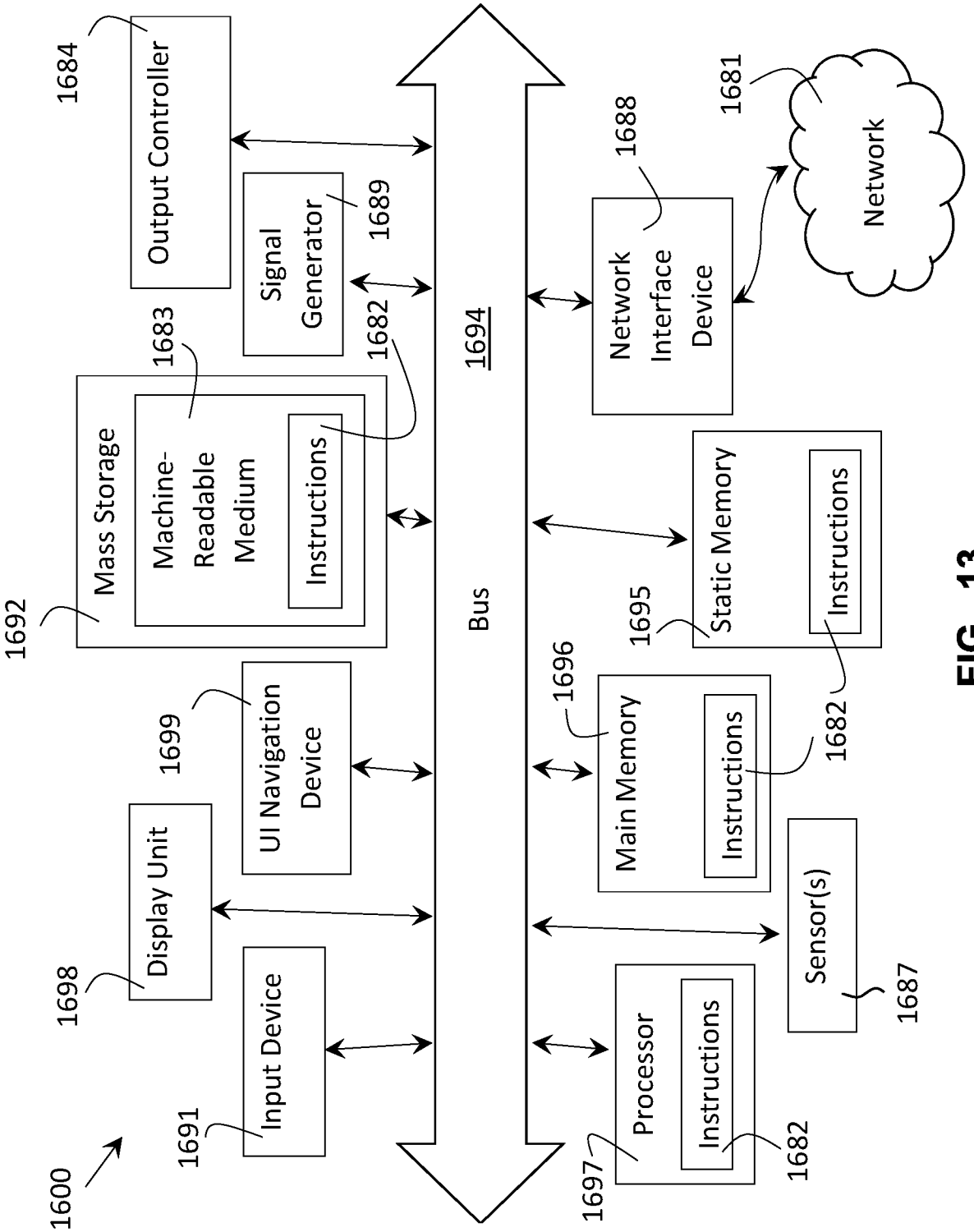
1600
1691
Input Device
1698
Display Unit
1699
UI Navigation Device
1692
Mass Storage
Machine-Readable Medium
1683
Instructions
1682
1684
Output Controller
Signal Generator
1689
1694
Bus
1697
Processor
Instructions
1682
1687
Sensor(s)
1696
Main Memory
Instructions
1682
1695
Static Memory
Instructions
1688
Network Interface Device
1681
Network

FIG. 13